Electronic Thesis and Dissertation Repository

11-19-2015 12:00 AM

Simulation of Magnetic Field Induced Current and Neuron Spiking for Magnetic Seizure Therapy

Abhijeet R. Wadkar
The University of Western Ontario

Supervisor
Professor Samuel F. Asokanthan
The University of Western Ontario

Graduate Program in Mechanical and Materials Engineering
A thesis submitted in partial fulfillment of the requirements for the degree in Master of Engineering Science
© Abhijeet R. Wadkar 2015

Simulation of Magnetic Field Induced Current and Neuron Spiking for Magnetic Seizure Therapy

(Thesis format: Monograph)

by

Abhijeet <u>Wadkar</u>

Graduate Program in Mechanical and Materials Engineering

A thesis submitted in partial fulfillment
of the requirements for the degree of
Master of Engineering Science

The School of Graduate and Postdoctoral Studies
The University of Western Ontario
London, Ontario, Canada

Abstract

Magnetic seizure therapy (MST) is currently on trial to treat severe cases of depression. This thesis is concerned with getting a deeper understanding of the mechanics behind MST by employing FEA of brain. The simulations performed via COMSOL helped identify the dimensions and coil types of the MST device as well as the angular probing orientations. Largest induced current due to the externally imposed magnetic field was found in the cerebrospinal fluid which was found to act as a barrier to induce current in the gray matter. In an attempt to relate the induced current to the neuron spiking, a mathematical model was selected for numerical simulation purposes. This model demonstrated the threshold adaptation of the neuron and also predicted the spiking process. These studies are envisaged to provide a more quantitative approach to virtually simulate the MST procedure and hence enhance the clinical trials that are currently underway.

Keywords: Magnetic Seizure Therapy, FEA, Electromagnetic induction, neuron spiking, threshold adaptation.

Acknowledgements

Table of Contents

List of Figures

List of Tables

List of Abbreviations

MST   Magnetic seizure therapy

FEA   Finite element analysis

ECT   Electroconvulsive treatment

CSF   Cerebrospinal fluid

ATP   Adenosine triphosphate

EEG   Electroencephalography

TMS   Trans-cranial magnetic stimulation

CAD   Computer-aided design

COMSOL   Multi-physics software

Chapter 1 Introduction

1.1 Background.

The human brain is one of the most complex organs of the body. It has millions of neurons (the cells in the brain) and billions of synapses (the gaps between each pair of neurons). The brain receives information from the sensory organs, and then processes this information and takes action according to the requirements of the situation. The human brain can also perform complex processes, such as thinking, memorizing and showing emotions. These are the advanced functions of the brain and these functions distinguish man from other species.

Neurology and psychiatry are the two disciplines of science that study the human brain. There is considerable overlap between the two. Neurology is the study of brain disorders with cognitive and behavioral abnormalities which have physical signs. Examples of such disorders are Parkinson's syndrome, stroke and multiple sclerosis. Psychiatry, on the other hand, is considered the study of mood and thought disorders which have no or minor physical signs. Examples of such disorders are depression, bipolar disorder and schizophrenia.

The first line of treatment for psychiatric illness is medication. But in acute cases where there is severe depressive episode, or manic episode in bipolar disorder and schizophrenia, the patient does not respond to normal medications. The patients can harm themselves or others during such situations. Electroconvulsive treatment (ECT) commonly known as 'shock treatment' needs to be given to the patient in such circumstances. This treatment was first introduced into the healthcare sector in the late 1930s. It is known that memory impairment has been found to be the severe side effect of this treatment although some minor ones also exist.

Psychiatrists have been trying to find techniques to mitigate or eliminate these side effects for many decades now. Over the last decade, they have found an alternative therapy called Magnetic seizure therapy (MST) to treat severe cases of depression which are traditionally administered via ECT. One of the key advantages of MST over ECT is that it has minimum side effects associated with memory loss. One of the primary objectives of this thesis is to get a deeper

understanding of the mechanics behind MST , in particular, the current induction in the brain due to externally imposed magnetic field. For this purpose, an attempt is made to virtually simulate the MST procedure. Finite element Analysis associated with electromagnetic stimulation within relevant parts of the brain and numerical simulation of the effect of electric current impulse on a neuron has been performed in order to fulfill this objective. In order to understand the mechanics behind these two processes, the present study is divided into two broad parts. The first part is the computer simulation of MST using the COMSOL software and the second part is a mathematical modeling and numerical simulation of the transmission of electric impulse into the neuron.

COMSOL Multiphysics® is a general-purpose software platform based on advanced numerical methods for modeling and simulation of coupled or multiphysics phenomena. In the present thesis, the Electromagnetic simulation available in the AC/DC module has been employed to simulate the MST procedure. But before discussing these sections of the thesis in detail, a brief introduction of the anatomy and physiology of the brain has been provided in this chapter.
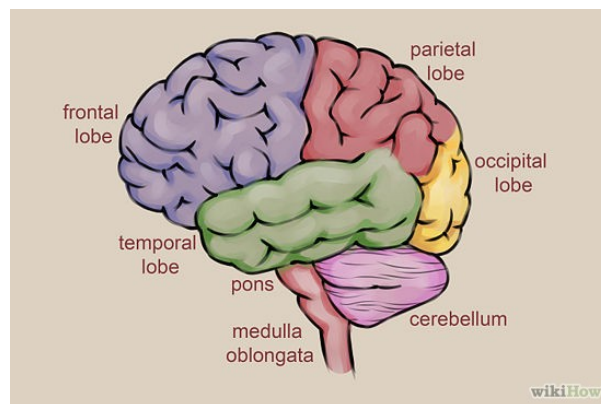
Figure 1-1 Parts of brain

Ref "Different Parts of Brain." Draw a Brain ~. Accessed May 31, 2015. http://paintingxxx.blogspot.ca/2013/05/draw-brain.html.

Brain anatomy and physiology: The main parts of human brain are the brain stem, cerebellum and the cerebrum. The brain stem consists of the medulla oblongata, the pons and the mid brain. It is concerned with breathing, circulation and digestion of food. The brain stem is responsible for routing information through the sensory nerves and the motor nerves. The function of the cerebellum is motor control, namely body motion and motion memory. The cerebrum which

consists of billions of neurons, are responsible for integrating and processing all the information coming into the brain. The outside of the cerebrum is called cerebral cortex. In addition, there are several other parts of the brain which are not described here in detail.

Cerebral cortex: This part of the brain, also known as the gray matter, resides on the outside of the cerebrum. The large grooves on the cerebral cortex are called fissures. The cerebral cortex is divided into four lobes: the frontal lobe, parietal lobe, temporal lobe and occipital lobe. The cerebral cortex is the most complex part of the nervous system, and plays an important role in expression of emotions. Positive emotions manifest in the left hemisphere and negative emotions in the right hemisphere. When exposed to positive situations, the left hemisphere of socially active children is activated to a greater extent than that of socially isolated children. By comparison, socially isolated children have more activity in the right hemisphere.
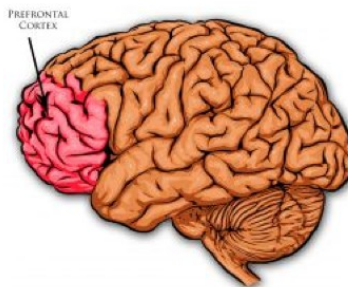
Figure 1-2 Schematic Representation of Prefrontal cortex

Ref: "Prefrontal Cortex." IAwake Technologies. Accessed May 31, 2015. http://www.iawaketechnologies.com/node/69.

Prefrontal cortex: This area is responsible for high order functions like language learning as well as general information processing and is extremely well developed in humans. This part of the brain is used for solving problems and making decisions. In the case of acute depression, the prefrontal cortex region of the brain is known not to function properly.
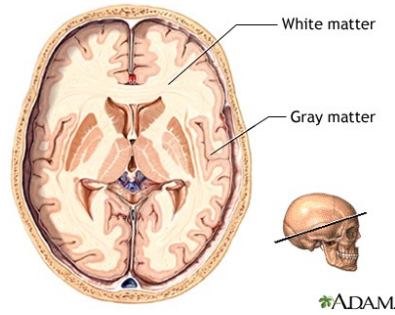
Gray and white matter: Gray matter has neurons and is mainly involved in thinking, cognition, etc. while white matter has axons, which carry messages to and from the brain. Cerebrospinal fluid (CSF) is present in the middle part as well as the periphery of the brain.

In the virtual simulation of MST proposed in the present thesis, some of the significant parts of the brain described above have been considered. In the electromagnetic simulation process, electrical conductivity values of the various regions have been employed in the prediction of induced current. In order that numerical predictions employing COMSOL can be effectively used for representing a virtual process of MST, an understanding of the neuron spiking process is also essential. Hence the literature review is divided into two major sections, namely, MST and COMSOL background and Mathematical Model of Neuron Spiking,

1.2 Literature review

1.2.1 MST and COMSOL background:

As mentioned briefly in the background section, the purpose of this thesis is to virtually simulate the MST procedure using the COMSOL software and also analyze the effect of electric current on the neuron. But prior to that, a literature review is conducted to gain more insight into MST and the ECT therapies as well as the advantages and disadvantages of each treatment. The literature review is not meant to give a biased positive view of MST because the fact remains that this treatment has been researched over the past 10 years only and is yet to be established for commercial use, whereas ECT has been in use since the 1930s and is still undergoing

development. This debate about which treatment will be better will continue until the safety and efficacy of MST is proven. The literature review of the thesis highlights this aspect of the current research in Psychiatry.

Even though efforts for developing ECT are on-going, there is still one significant drawback to this treatment, namely memory loss. Psychiatrists claim that MST can have the same positive effect of ECT with much less memory loss. According to (George Kirov, et.al, 2008)), patients returned to a normal state in a shorter period of time after the MST treatment session than that of the ECT session. This is called the recovery time period and it was shorter by 15 minutes 35 seconds for MST than that for ECT. The obvious consequence of this was that patients suffered less memory loss when they underwent MST as compared to ECT. But the paper also highlighted a drawback that seizures cannot be induced in patients with certainty using the MST equipment.

This drawback has also been highlighted in the website of Magventure, a Denmark based company which manufactures this equipment (Magnetic Seizure Therapy. (n.d.). Retrieved August 22, 2015, from http://www.magventure.com/en-gb/Researchers/Applications/Magnetic-Seizure-Therapy). Hence it can be concluded from these two sources that inducing seizures in patients is more of technical problem rather than a medical problem and research companies are making good progress in this regard by collaborating with psychiatrists.

Another interesting concern about MST is the effect of the strong electromagnetic field on the human body. (Magda Havas, 2004) in her paper has highlighted the fact that even ultra low frequency fields of the magnitude of micro-Tesla can cause lymphoma and nervous system tumors in the body. The magnetic field intensity produced in MST is up to 2 Tesla at 100 Hz and such a strong magnetic field may cause serious effects on the human body. According to the author, this has to be definitely investigated before MST treatment could be brought under commercial use. But the author admits that the prospects of side effects might not be serious as there are two camps of scientists who have opposite views of the effects of ultra low electromagnetic fields on the human body. The side effects that have been discovered in the paper are not proven and are mere observations which are very rare and random.

After reviewing these papers which highlighted the drawbacks of MST treatment, a paper written by (Sarah Kayser, et. al, 2010) has been reviewed. These researchers did an open label study of patients suffering from treatment major depression, which was not psychotic. Twenty patients underwent trials in this research project. As per their expectations, these authors found out that the positive effects of MST are comparable to that of ECT. Even though the study involved small sample size of patients, this conclusion of the paper was enough to start our study of MST.

The inspiration of doing the COMSOL simulation of the MST procedure has been derived after reviewing a paper written by (Zhi-De Deng, et.al, 2010). The research performed in this paper was a collaborative work between the Department of Electrical Engineering of the Columbia University and psychiatrists at the Duke University and Columbia University. A clue of application of Engineering in Psychiatry has been taken from this paper. These researchers have carried out a Finite element Analysis of the ECT and MST procedures using the commercially available ElecNet and MagNet software. In this analysis, the researchers have modeled the brain as a sphere having concentric layers representing different tissues of the brain. The results that they obtained proved that MST had a superficial and focal effect on the brain as compared to ECT. It was speculated from these results that there will be less cognitive side effects on the brain due to MST as compared to ECT and this was found out to be in accordance with the clinical trials of MST.

Thus it could be considered that MST was a good alternative to ECT and would be appropriate to study the mechanics of MST via a suitable numerical tool. For this purpose, the COMSOL software has been used and the idea of the spherical head model proposed by Zhi-De Deng, et.al (2010) has been adopted for the present study. These researchers had the manufacturer's data, X-rays and inductance measurements to model the magnetic coil used in MST. But as there was no such data available for the present study, the coil has been modeled as a simple electromagnet using a copper wire winding and the FEA analysis has been performed to determine the maximum current density and its location in various layers of the brain model.

1.2.2 Mathematical Model of Neuron Spiking

Ideally, this study required a mathematical model of the human neuron. However, within the limited framework of time, a paper (Bertrand Fontaine, et.al, 2014) which showed the effect of electric current of random nature on the sensory neuron of a barn owl has been reviewed. This paper provides an initial guide to perform the investigation proposed in the present study. The research presented in the paper consists of conducting experiments on a barn owl by subjecting its ears, through headphones, to a noise signal of a certain broadband. The results of the experiments were then described by a deterministic mathematical model, which predicted when the neurons would spike. This model did not mention about the nature of transmission of electric impulse but only commented on the prediction of the occurrence of the phenomenon.

Although it had been accepted that the prediction of spiking of the neurons was a deterministic process, it had to be determined whether the nerve impulse transmission was deterministic or stochastic. Hence a paper (John A. White, et.al, 2000) which discussed about the stochastic nature of transmission of electric impulse through the neuron was reviewed. This paper gave a different insight to the present research problem. In this research, the responses of the node of Ranvier from a sciatic nerve of the frog were recorded and it was found out that the transmission of electric impulse through the nerve is stochastic in nature. But an interesting fact was mentioned in the paper that the nature of transmission of electric impulse through the nerve, whether it is deterministic or stochastic, depends on the number of channels present in the neuron. As the number of channels in the neuron increases, the process becomes more deterministic. But a large amount of energy is required in the form of ATP (Adenosine triphosphate) molecules is required for the functioning of the Sodium-Potassium pump, which maintain the membrane potential of the neuron. The reliability of transmission of information through the neuron depends on the number of channels present in the neuron.

After reviewing these two papers, it was certain that different species would have either a deterministic or stochastic nature of nerve impulse transmission depending on its metabolic capacity. The deterministic model has been chosen for our simulation because it showed the deterministic nature of the neuron when it was subjected by a random input current.

7

1.3 Clinical procedure of MST:

In order to relate the findings of the present thesis to the medical practice of this therapy, the clinical procedure of MST has been briefly mentioned in this section. The Magventure website(Magnetic Seizure Therapy. (n.d.). Retrieved August 22, 2015, from http://www.magventure.com/en-gb/Researchers/Applications/Magnetic-Seizure-Therapy) provided a very good description of the clinical procedure of MST. Hence it has been quoted from the website in a point wise manner as follows:

- Seizures were elicited under general anesthesia (propofol).
- The patient was oxygenated during anesthesia with 100 % O_2.
- The motor activity of the right foot is assessed visually in order to track the duration of motor seizures and bilateral frontal-mastoid EEG recordings are obtained by an EEG device.
- Treatments are delivered with a magnetic stimulator (MagVenture MagPro MST) using the highly efficient "Twin Coil".
- Stimulation repetition rate 100 pps (pulses per second). Number of pulses: 100-600 (duration 1-6s)
- Stimulation amplitude of 100%.
- During the stimulations, the center of the coil is placed at the vertex.
- The peak magnetic field induced above 2 Tesla at the coil surface.
- Two MST sessions per week.

The technical parameters of MST and ECT equipment have also been compared. This comparison has been summarized in a tabular form as follows:

Properties	ECT	MST
Waveform	Bipolar, brief current pulse, square wave	Biphasic waveform, dampened cosine waveform
Duration of stimulation	5-8 seconds	Max 6 seconds
Type of coil		Twin coils each of 13 cm diameter, circular coil, cap coil and so on.

Stimulation		Stimulation frequency was 100 Hz and train duration up to 6 s.
Repetition Rate		Repetition Rate was from 0.1 to 250 pps. To obtain comparability
Pulse width	0.5 milliseconds	0.37 milliseconds
Pulse amplitude	less than 800mA	much less than ECT value
Voltage	450V	
Electric charge/ magnetic field	540mC – 1000mC	2 Tesla
Number of sessions	6-12 sessions in total with 2 sessions per week	6-12 sessions in total with 2 sessions per week

Table 1-1 Comparision of technical parameters of ECT and MST

1.4 Scope and motivation of thesis

As mentioned in the background section, the intent of the present thesis is to study an alternative treatment for ECT used for treatment resistant depression. ECT has been developed in the 1930s and is still the most effective form of treatment for acute depression. But it has memory loss as a serious side effect. Psychiatrists have been trying for decades together for reducing this side effect of ECT and they have achieved it to some stage. But still there exist some noticeable side effect of ECT. As time has progressed, psychiatrists have also come up with some creative ideas which would be an alternative for ECT. The new dimensions of research to find an alternative for ECT can be broadly classified as "Invasive neuro-stimulation techniques" and "Non-invasive neuro-stimulation techniques".

The examples of "Invasive neuro-stimulation techniques" are Vagus nerve stimulation, Cortical brain stimulation and Deep brain stimulation. All these techniques require surgeries to be performed on the brain. This makes them complicated and studying the research in this area would require extensive knowledge from the field of medicine. Hence studies in this direction have been excluded from this thesis.

The examples of "Non-invasive neuro-stimulation techniques" are Repetitive trans-magnetic stimulation, Magnetic seizure therapy, trans-cranial direct current stimulation and some others. Among all these new evolving techniques, Magnetic seizure therapy is the one which closely resembles the procedure of ECT and therefore has similar positive effects but with less or insignificant side effects. MST procedure can be simulated via Finite Element Analysis and useful insights can be provided by the engineers to the medical fraternity.

The goal of this thesis is to virtually simulate the clinical procedure of MST. The first part of the investigation deals with Finite element analysis of MST using the COMSOL software. During this analysis, the human head is represented by a sphere having concentric layers. The different layers consist of representation of scalp, skull, cerebrospinal fluid, gray matter and white matter. The conductivity properties of each material are applied to their respective layer. The alternating magnetic field is produced by an electromagnet, consisting of copper wire. This modeling is far from reality but it has been used because the technology, by which 1T magnetic field is produced when the coil is placed in close vicinity of the brain, has not been public until now. The current is induced in the brain from the magnetic field produced by the powerful electromagnets used in the MST equipment has been found out by the Finite Element Analysis procedure. The virtual simulation of the procedure would have been completed only when it is found out whether this induced current is sufficient to activate the neurons in the prefrontal cortex. This is because it is known from fundamental studies of psychiatry that during severe depression, the neurons in the prefrontal cortex become inactive.

Hence the second part of the thesis is to determine a mathematical model of neuron which would take the current induced by the simulation as input. The mathematical model can then be simulated using Simulink and the response of the neuron could predict whether it has been activated or not. Ideally, a mathematical model of a human neuron should have been employed for simulation purposes. But within the given timeframe of research work, a deterministic mathematical model showing the neuron spiking of the sensory nerves of a barn owl has been selected for the simulation. This model does have some resemblance to our requirement. It shows the response of the neuron to a broadband noise signal applied to the ears of the owl. This noise

is converted in to current by the sensory organs, which was given as an input to the mathematical model.

It may be noted that an apparent disjoint between two parts of this thesis exists. The first one involves the calculation of the induced current in the human brain while the second part involves determining the neuron spiking of a barn owl subjected to a stochastic input current signal. However, when the barn owl study is extended to the neuron spiking in humans or from other models available within the mathematical neuroscience community, such a linkage of psychiatry and theoretical neuroscience could be carried out in the future and its results can be verified by psychiatrists.

1.5 Thesis Outline

Chapter 1 introduces the thesis topic to the reader. The scope and objectives of the thesis are defined in a section of this chapter. It consists of virtual simulation of the MST procedure and mathematical modeling of a neuron. But in order to understand this, a brief introduction to the brain anatomy and physiology has been provided. Literature review of the MST has been carried out in order to justify the scope and objectives of the thesis. Before starting with the FEA of the human brain, the clinical procedure of MST has been studied so that it is understood in a better manner.

Chapter 2 deals with the FEA of the human brain using the COMSOL software. The brain has been represented as a sphere having concentric layers. Each layer represents a separate tissue of the brain and is assigned appropriate conductivity properties. Simulations have carried out in order to find out the dimensions of a single layer coil. After that several parameters are varied and the performance of the coils has been evaluated. The next part of this chapter involves the simulations of the different configurations of the coil, namely, cap coil, double stacked coil and multi-stacked coil. A comparative study of the performance of the different coil configurations has been carried out and this study yields the fact that the multi-stacked coil is the most effective and the double stacked coil is the least effective amongst all of them.

Chapter 3 involves the study of the mathematical modeling of the neuron. The neuron anatomy and physiology has been discussed in the first part of this chapter to prepare an initial background of the mathematical modeling. In this part, the concepts of action potential, nerve impulse transmission and its related topics have been explained in detail. A deterministic mathematical model of a barn owl, involving three non-linear coupled differential equations has been selected to show the effect of random noise on the neuron. The concept of threshold adaptation has been discussed in the last part of the chapter.

Chapter 4 summarizes the conclusions and recommendations of the thesis. It has been concluded that a spherical model with concentric layers can be used to represent the human brain by conducting its FEA. The largest amount of current is observed in the cerebrospinal fluid at an orientation of 45° with respect to the vertical axis. The current in the cerebrospinal fluid acts as a barrier to induce current in the gray matter. Mathematical modeling of the neuron yields the explanation of the concept of threshold adaptation very well. This chapter concludes with the recommendations for the future work. They include finding out a mathematical model of the human neuron and then linking psychiatry and theoretical neuroscience for the purpose of the virtual simulation of MST. The option of using other advanced software should be explored in order to improve the simulations of the brain. MST device technology should be improved so that more current is induced in the gray matter of the brain.

1.6 Closure

This chapter summarizes and provides the preliminary knowledge that is required for carrying out this research project. The discussion of brain anatomy and physiology is important as this thesis involves the application of Finite Element Analysis (FEA) of the human brain. The literature review gives the reader a balanced view of the advantages and disadvantages of MST. After that the clinical procedure of MST gives an insight of this therapy as viewed by the psychiatrists. The section of scope and objectives reveal that this thesis is about doing a virtual representation of the MST procedure. This have been done in two parts, namely, FEA of the human brain which gives the current induced in the brain and mathematical modeling of the neuron which will show whether the neuron is spiking when a current is applied to it. Finally, the thesis outline gives the overall view of the different chapters of the thesis.

Chapter 2 COMSOL Simulation of MST

2.1 Introduction

This chapter involves the study of the virtual simulation of the MST procedure using the COMSOL software. The human head is modeled by a concentric layered sphere, each layer having properties equivalent to different tissue of the brain. This model has been validated by the research group of Sara Kayser and Zhi-de Deng of the Columbia University. These researchers have conducted clinical trials and found that the model fairly represents the human head. A 2-D axis-symmetric feature of the COMSOL software has been used for the simulation in order to make use of the symmetry of the head model and the coil. In the beginning, the geometric dimensions of the coil have been found out in order to produce approximately 1 Tesla of magnetic field density. After fixing the coil dimensions, detailed simulations have been carried out for the single layer coil configuration. The frequency of input current to the coil has been kept as 100 Hz and the input voltage has been set to 50V in order to produce a maximum magnetic field density of 1.07 Tesla. This simulation gives the current density in different layers of the brain. The current in a specific layer of the brain is then found out by multiplying the current density by the area of the prefrontal cortex region. It has been found out from this simulation that the current is maximum in the cerebrospinal fluid. Several coil parameters of the single layer circular coil have been varied in order to analyze its performance and draw relevant conclusions from the simulation data. One of the conclusions is that probing of the results has been most effective when done at an angle of 45° with respect to the vertical axis. The variation of the magnetic field density vs. the frequency and the variation of magnetic field density vs. input voltage have been studied. It has been found out that the magnetic field density rapidly diminished as the frequency of the input voltage increases. It has also been found out that the variation of magnetic field density vs. input voltage is most prominent when the frequency of the coil excitation is 100 Hz.

After that, simulations have been carried out for other configurations, namely, cap and multi-stack coil. It has been proved that the current induced in different layers of the brain is maximum when probed at an angle of 45° with respect to vertical axis. Hence the probing has been done

only this orientation for further simulations. It has been shown that the multi-stack coil produces maximum amount of induced current at the least input voltage given to the coil and the double stack coil produces the least amount of induced current in the brain for a magnetic field density of approximately 2 Tesla. Hence it has been concluded that multi-stack coil is the most effective amongst all the configurations discussed in this research and the double stack coil is the least effective. The detailed results have been discussed in the following sections of this chapter.

2.2 COMSOL Simulation Procedure

The Magnetic and Electric fields physics interface of the AC/DC module of the COMSOL software has been used to simulate the Magnetic Seizure Therapy (MST) procedure. In the present simulation study, the human brain has been modeled by a concentric layered sphere having thickness and conductivity properties equivalent to its relevant tissues, which is shown in Figure 2-1. This equivalence has been demonstrated in many studies and has been documented in the paper by (Zhi-De Deng, et.al, 2010). The equivalent sphere having concentric layers representing anatomically realistic head model has been widely accepted and also been used in previous computational investigation of (Trans-magnetic Stimulation)TMS and ECT (see, e.g., Sekino M, Ueno S., 2002). For simulation purposes, the sphere radius has been taken as 0.084m based on the study by (K M D Bushby, et.al, 1992) in which the circumference of an average human head has been mentioned. The radii, thickness and the conductivity values of the respective layers have been summarized in Tables 2-1 and 2-2. Further, in order to identify the layers associated with the regions of interest a simple color code has been adopted as illustrated in the tables.
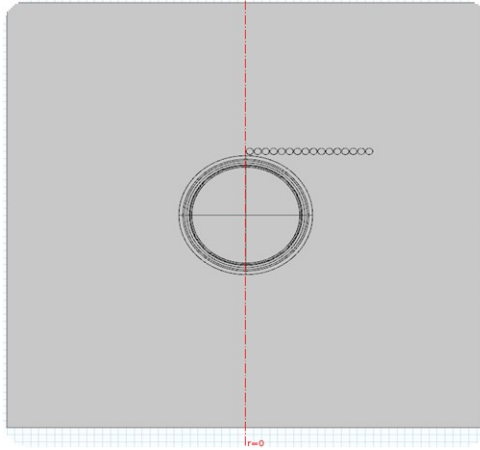
Figure 2-1: COMSOL geometry of the MST model, with coil and concentric sphere.

Layer Name	Dimensions (m)	Thickness (m)
Scalp	0.084	0.005
Skull	0.084 - (0.00708)	0.00708
Cerebrospinal fluid	0.084-(0.00708+0.003)	0.003
Gray Matter	0.084-(0.00708+0.003+0.003)	0.003
White Matter	0.0678	0.0677

Table 2-2: Dimensions used to model the concentric sphere, and the thickness values for each layer.

Layer Name	Properties (Condictivity S/m)
Scalp	0.33
Skull	0.0083
Cerebrospinal fluid	1.79
Gray Matter	0.33
White Matter	0.14

Table 2-3: Five layers and the electrical conductivity value for each layer.

The coils of the MST device are represented by simple electromagnetic coil with several configurations where one such configuration (single-layer circular) is illustrated in Figure 2-1. In all coil configurations considered in the present study, input sinusoidal voltage amplitude of 50 V has been set in order that a magnetic field in the neighborhood of 1 Tesla can be achieved at the coil surface. Further conforming to the MST procedure, all comparison studies have been performed with an input frequency of 100 Hz, although some preliminary studies with varying frequencies have been performed for justification of the COMSOL predictions. After some trial studies using various combinations of geometric parameters for the coils, a coil having 16 windings with a wire diameter of 9 mm and spacing of 1mm between the two concentric circles of the coil has been found suitable for producing a magnetic field of around 1 Tesla. Once the coil dimensions are set, several simulations have been carried out by varying voltage magnitude and frequency in order to predict the performance of various coil configurations.

A 2D axis-symmetric configuration available within the software has been chosen to simplify the modeling process of the coil. Different configurations of the coil have been tried out, which were of 2D axis-symmetric nature, namely the cap coil, double stacked coil and the triple stacked coil. After the simulations are done, induced current density values, in different layers of the sphere, are recorded along the vertical/horizontal axis and 45° with respect to the vertical axis. The electric current has also been calculated from the induced electric current density, in different layers of the sphere. The maximum current induced in different layers have been predicted by multiplying the current density with the prefrontal cortex area.

2.3 Single-layer Circular Coil

As mentioned in the previous section, a voltage of 50 V has been applied to a single layer copper coil, the frequency is set to a value of 100 Hz, and the simulation is computed. Figure 2-2 shows a single layer coil configuration. After the simulation has been run, the maximum magnetic flux density recorded is 1.07 Tesla and its plot, generated by COMSOL has been displayed in Figure 2-3.
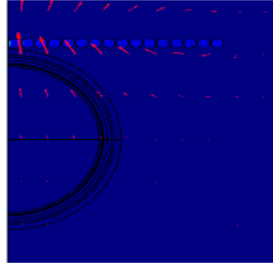
Figure 2-2: Single coil with multiple turns consisting of 16 windings.
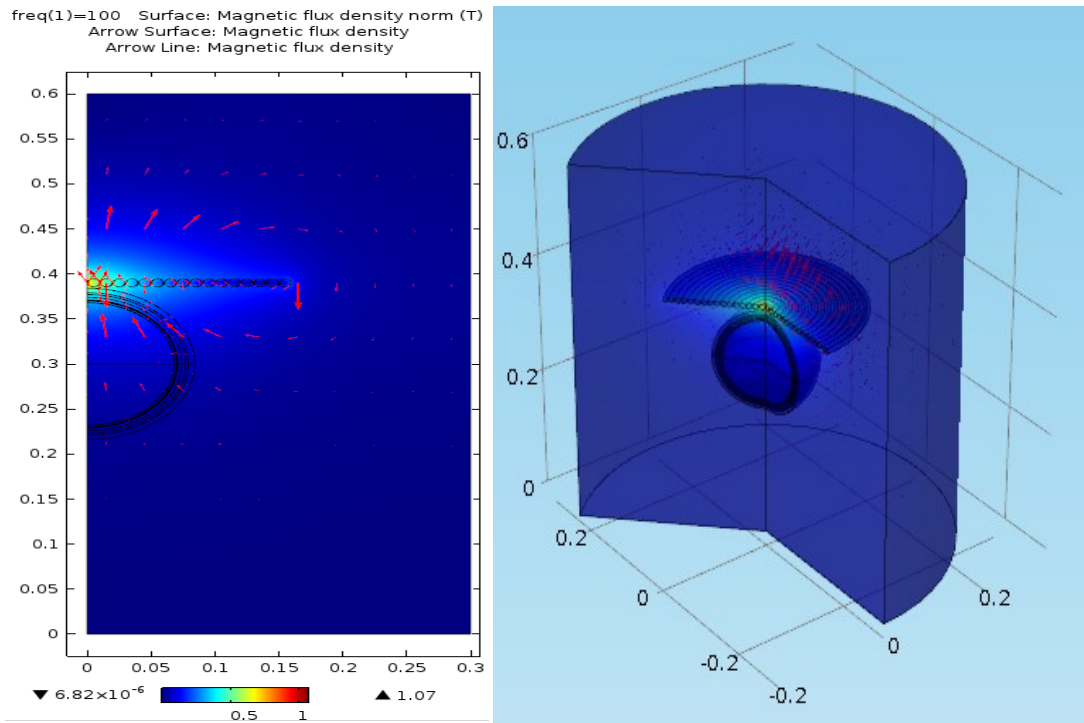
Figure 2-3: Axis-symmetric Magnetic Flux Density plot of MST.
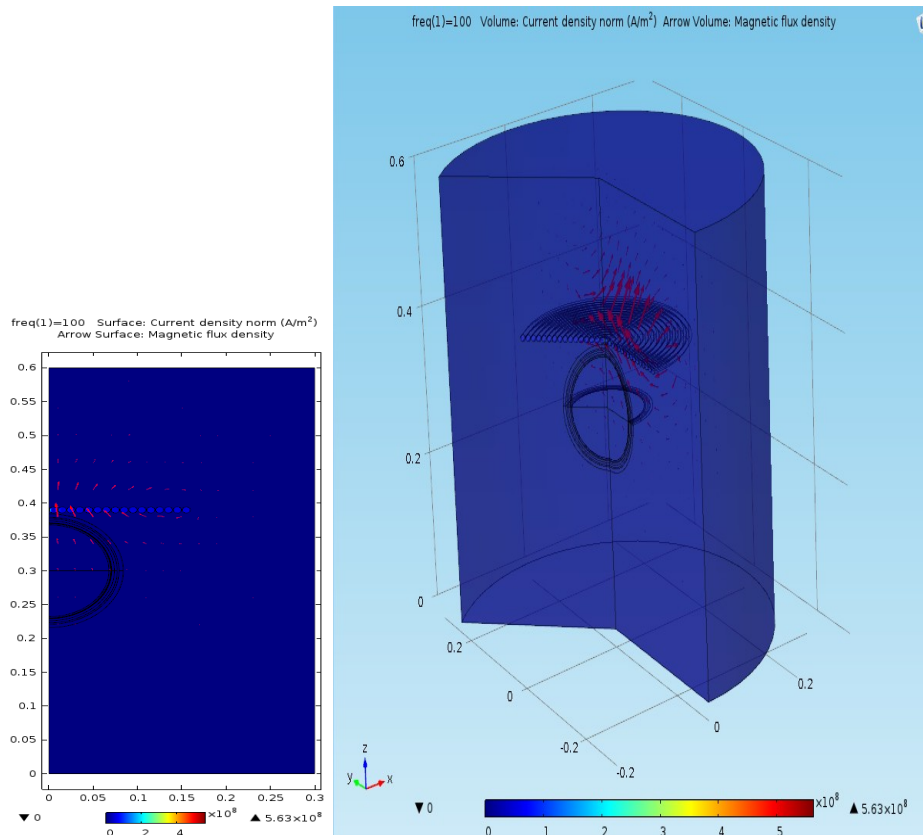
Figure 2-4 Current density in the coil and the brain.

Figure 2-3 shows that the peak magnetic flux density is 1.07 Tesla. Figure 2-4 shows the distribution of the current density within the brain. Its value is very high at the coil surface. But we are concerned with the current density in the brain. Hence this will be discussed in the future sections.

2.3.1 Angular probing

The subsequent procedure of the simulation consist of probing the current density induced in the brain along the vertical, horizontal and an axis 45° with respect to vertical axis. After probing the current density, the current in the different layers of the brain has been found out by the multiplying it with the area of the prefrontal cortex which is approximately equal to 0.0229 m^2 (A new Canadian brain therapy targets depression. (n.d.). Retrieved August 22, 2015, from http://www.theglobeandmail.com/life/health-and-fitness/health/a-new-canadian-brain-therapy-targets-depression/article5212749/). Figure 2-5 shows the table having values of induced current at different locations in different layers of the brain probed at along the vertical axis. It can be

18

observed from Table 2-2 that the conductivity value of cerebrospinal fluid (1.79 S/m) is the highest amongst all the layers of the brain. Hence the maximum current is induced in this layer of the brain. This has been shown by the graph in Figure 2-6. But here it can be noted that the values of the current induced at this orientation is negligible and is not of our interest.

Layer	Position on graph	Current Density (A/m^2)	Current In that area (A)
Scalp	1	0.003985	9.12565E-05
	2	0.003989	9.13481E-05
	3	0.008013	0.000183498
	4	0.003545	8.11805E-05
	5	0.003538	8.10202E-05
Skull	7	8.16E-05	1.86871E-06
	8	8.16E-05	1.86818E-06
	9	8.14E-05	1.86314E-06
	10	7.99E-05	1.82902E-06
	11	7.99E-05	1.82971E-06
Cerebrospinal Fluid	13	0.01629	0.000373041
	14	0.01628	0.000372812
	15	0.01627	0.000372583
	16	0.01578	0.000361362
	17	0.01578	0.000361362
Gray Matter	19	0.002737	6.26773E-05
	20	0.005829	0.000133484
	21	0.002737	6.26773E-05
	22	0.002631	6.02499E-05
	23	0.005604	0.000128332
White Matter	25	0.00352	0.000080608
	26	0.0023001	5.26723E-05
	27	0.001046	2.39534E-05
	28	0.0010303	2.35939E-05
	29	0.0010079	2.30809E-05

Figure 2-5: Axisymmetric Model of the location (highlighted in lime green) where the data was sampled for the five different layers.

Figure 2-6: Graph illustrating the varying current at different locations within different layers of the brain.

Layer	Position on graph	Current Density (A/m^2)	Current In that area (A)
Scalp	1	1.2177	0.02788533
	2	1.2176	0.02788304
	3	1.1974	0.02742046
	4	1.1612	0.02659148
	5	1.1257	0.02577853
Skull	7	2.76E-02	0.00063204
	8	2.77E-02	0.000633414
	9	2.73E-02	0.000624483
	10	2.72E-02	0.000622422
	11	2.61E-02	0.00059769
Cerebrospinal Fluid	13	5.661	0.1296369
	14	5.6256	0.12882624
	15	5.5495	0.12708355
	16	5.4866	0.12564314
	17	5.435	0.1244615
Gray Matter	19	0.9769	0.02237101
	20	0.9622	0.02203438
	21	0.9514	0.02178706
	22	0.9428	0.02159012
	23	0.9298	0.02129242
White Matter	25	0.3875	0.00887375
	26	0.3799	0.00869971
	27	0.3757	0.00860353
	28	0.3705	0.00848445
	29	0.3648	0.00835392

Figure 2-7: Axis-symmetric Model of the location (highlighted in lime green) where the data was sampled for the five different layers.

Figure 2-7 illustrates an important orientation at which the current is probed. It has been observed that the current in all the layers of the brain is higher as compared to the vertical orientation. A repeated observation is that the value of current is maximum in the cerebrospinal fluid. Its maximum value is 128mA. The current used in the ECT is of the magnitude of around 800mA. Hence this value is comparable to the current in ECT and is expected to be correct.

Figure 2-8 shows the data analysis of the table in Figure 2-7 in graphical form. A striking observation can be made from the data that has been acquired until now. It is difficult to induce a current which penetrates the cerebrospinal fluid and thereby affect the gray matter. This is important to achieve because the MST treatment is used to stimulate the neuron in the gray matter of the prefrontal cortex and not the cerebrospinal fluid. This observation is repeated in all the simulations and will be discussed further in the last section of this chapter.
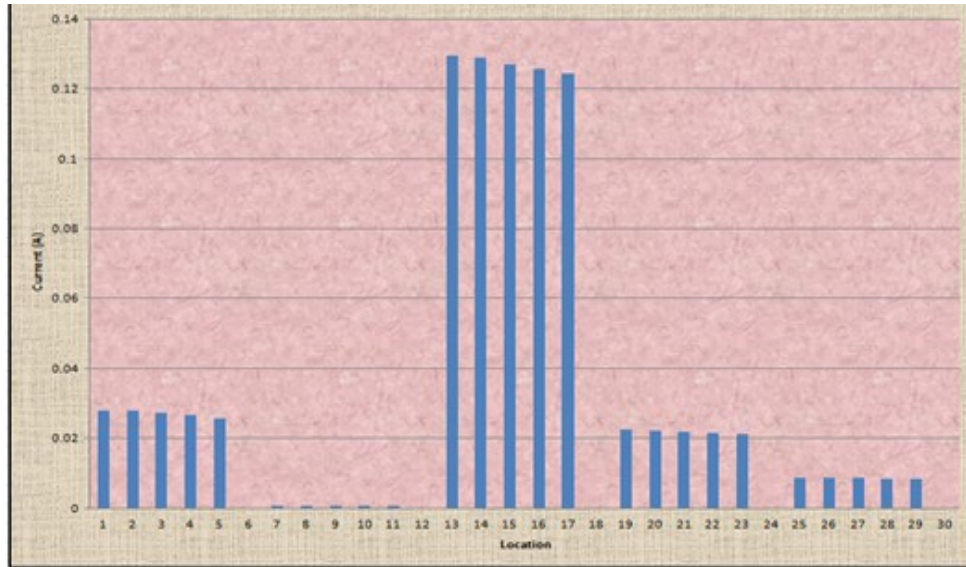
Figure 2-8: Graph illustrating the varying current at different locations within different layers of the Brain

Figure 2-9 shows the results obtained by probing the values of current at horizontal axis orientation. The value of current induced in the cerebrospinal fluid is around 63 mA which is lesser than the 45° orientation condition but greater than the vertical axis orientation. Figure 2-10 shows the results of this simulation in the graphical form.

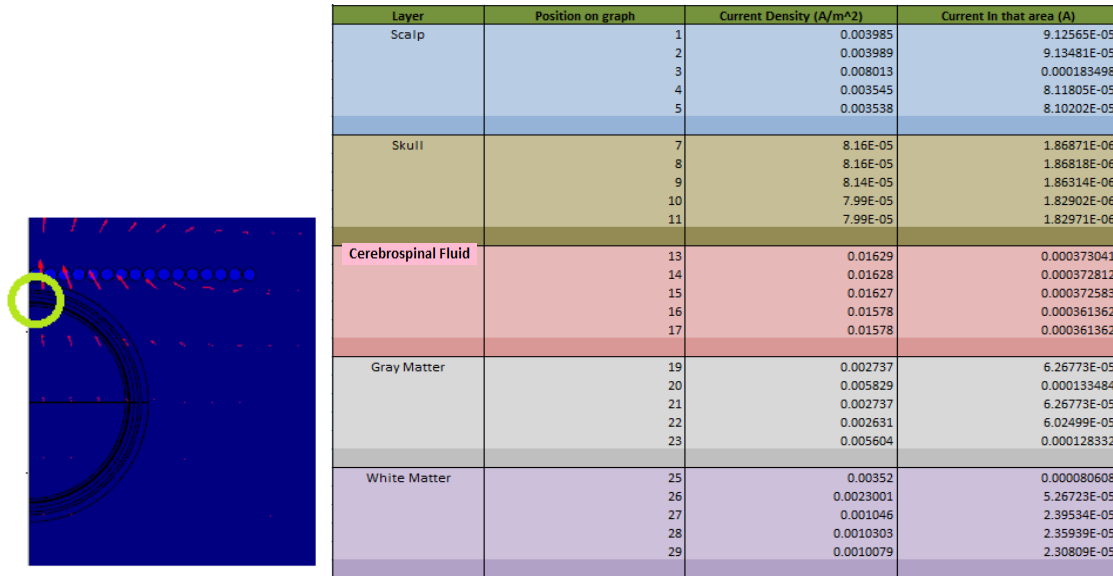| Layer	Position on graph	Current Density (A/m^2)	Current In that area (A)
Scalp	1	0.5387	0.01233623
	2	0.5354	0.01226066
	3	0.5344	0.01223776
	4	0.5302	0.01214158
	5	0.5278	0.01208662
Skull	7	1.29E-02	0.000295639
	8	1.30E-02	0.000297929
	9	1.30E-02	0.000297242
	10	1.29E-02	0.000296326
	11	1.29E-02	0.000295639
Cerebrospinal Fluid	13	2.772	0.0634788
	14	2.761	0.0632269
	15	2.745	0.0628605
	16	2.734	0.0626086
	17	2.723	0.0623567
Gray Matter	19	0.4999	0.01144771
	20	0.4977	0.01139733
	21	0.4944	0.01132176
	22	0.4918	0.01126222
	23	0.481	0.0110149
White Matter	25	0.2069	0.00473801
	26	0.2062	0.00472198
	27	0.2044	0.00468076
	28	0.2036	0.00466244
	29	0.2029	0.00464641
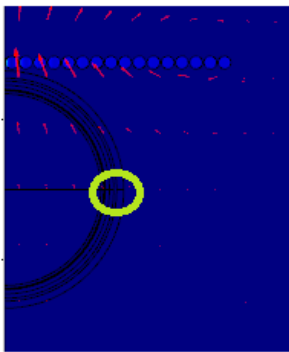
Figure 2-9: Axisymmetric Model of the location (highlighted in lime green) where the data was sampled for the five different layers.
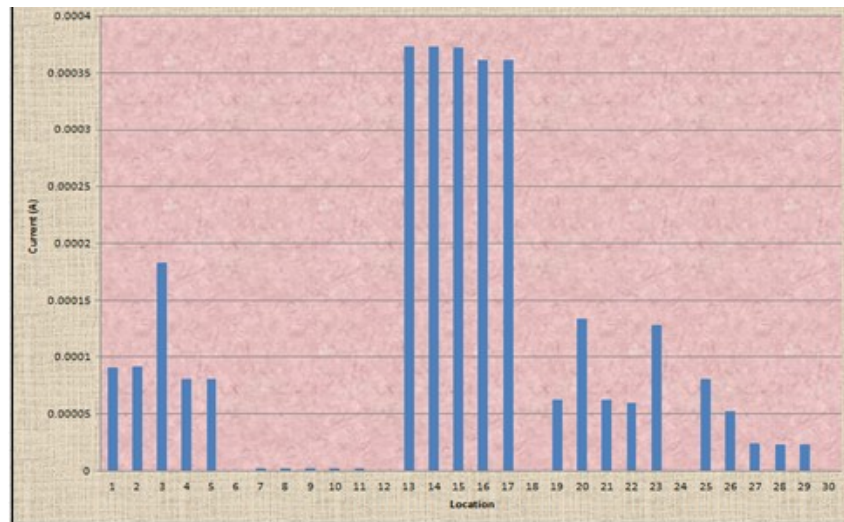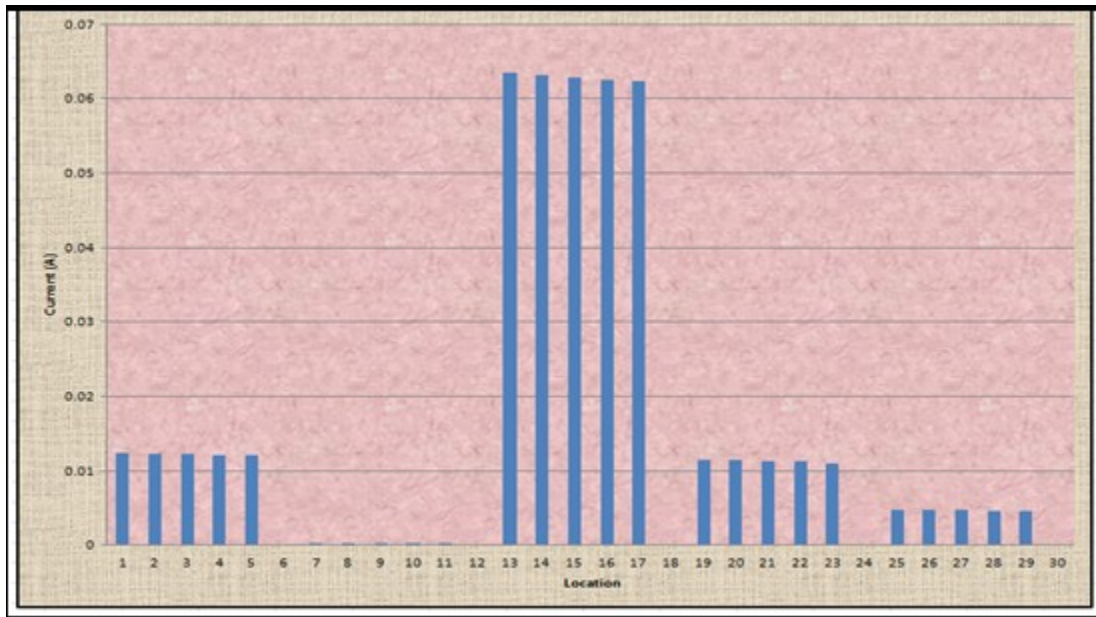
Figure 2-10: Graph illustrating the varying current within different layers of the Brain, and sampled at the location shown in figure 9.

After analyzing the simulation data it has been found out that the optimum probing can be done at 45° orientation with respect to the vertical axis. Hence while studying the different coil configurations such as the cap coil and the stacked coil, only the data corresponding to the 45° orientation case shall be reported in the thesis although the data has recorded for all three orientations in other types of coils.

2.3.2 Varying Frequency and Voltage Study

The next step in the simulations of the single layer circular coil involved studying the variation of magnetic flux density when the frequency and magnitude of the input voltage was varied. The frequency of the input voltage, which has set at a constant magnitude of 50 V, has been varied from the practical value of 100 Hz to an arbitrary value in the range of radio frequency, 1000000 Hz. Figure 2-11 shows the variation of the magnetic flux density (T) vs. the logarithmic scale of the frequency (Hz). The graph shows that the magnetic flux density drastically reduces as the frequency of the input voltage increases. This shows the logic used by the technologists in developing a device which produces an ultra-low frequency magnetic field. Table 2-3 shows the data recorded in the tabular form.
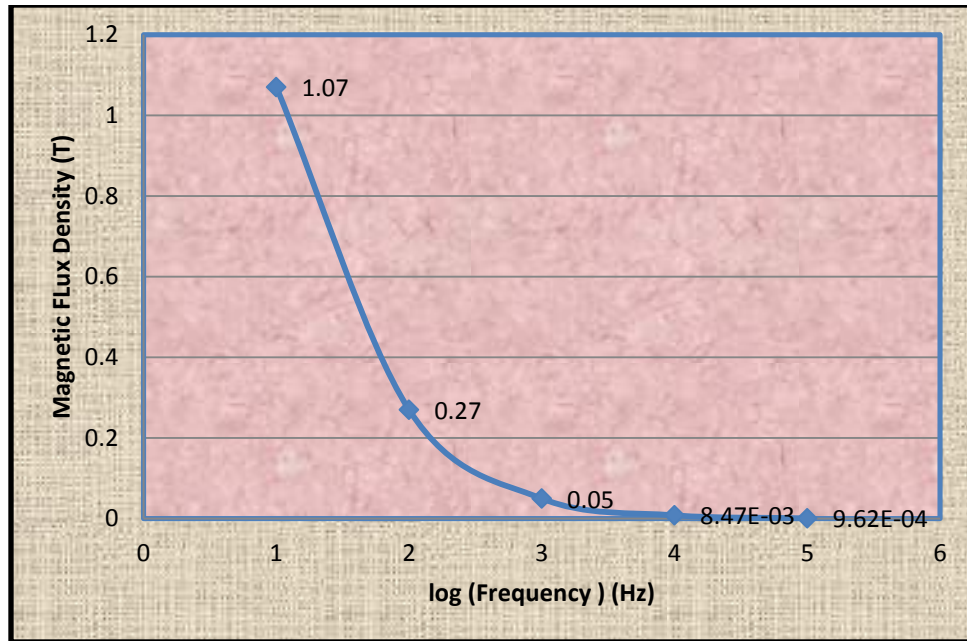
Figure 2-11: Graph illustrating the peak magnetic flux density at 50 V and the frequency in logarithmic scale.

Frequency (Hz)	Peak Magnetic Flux Density (T)	Logarithmic value of Frequency
100	1.07	2
1000	0.27	3
10000	0.05	4
100000	8.47E-03	5
1000000	9.62E-04	6

Table 2-3: Values used to graph figure 2-13.
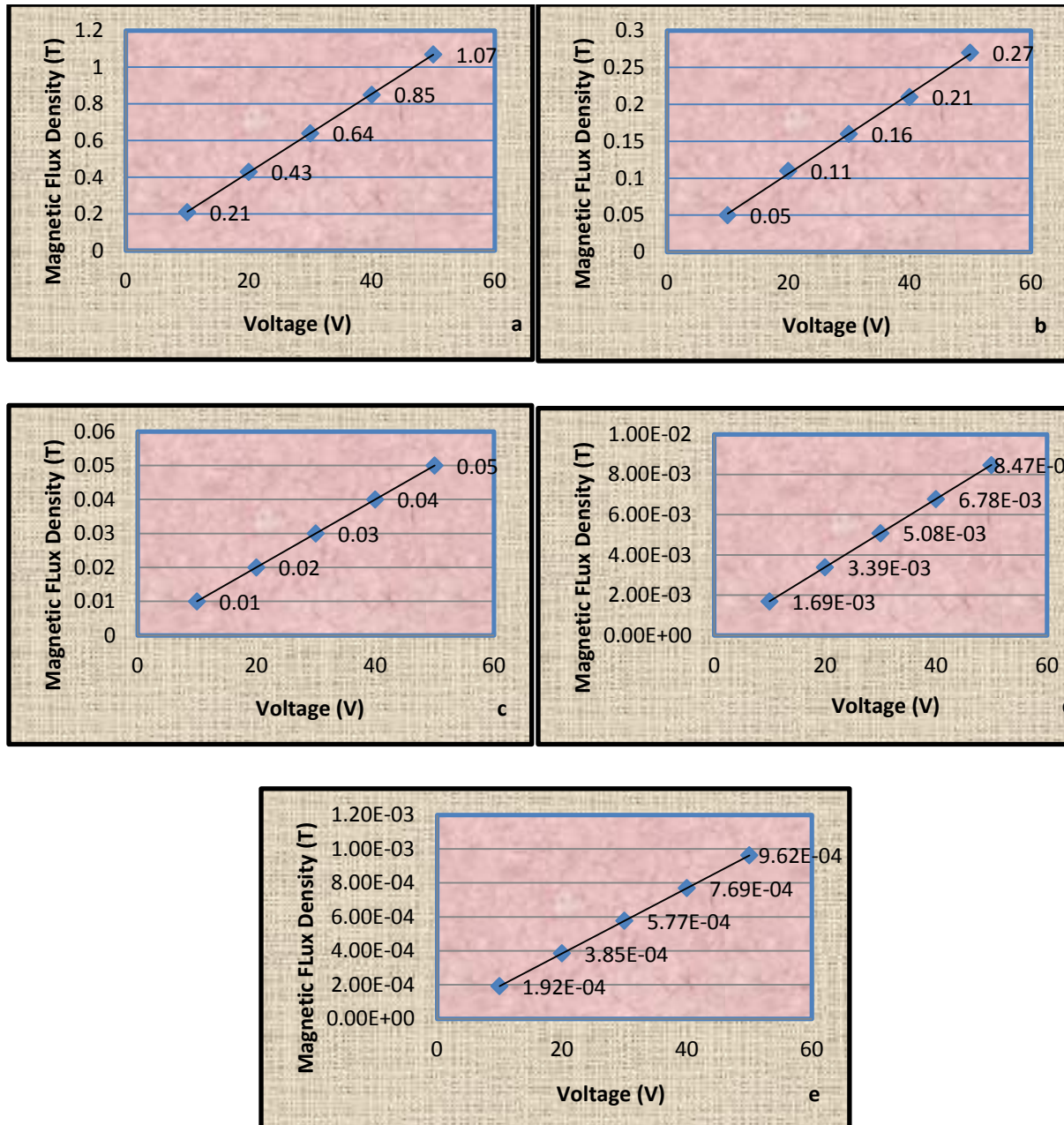
Figure 2-12: Graphs a, b, c, d and e display the magnetic flux density vs. voltage for 100 Hz, 1000 Hz, 10000 Hz, 100000 Hz, and 1000000 Hz respectively.

Figure 2-12 shows the variation of Magnetic flux density (T) vs. voltage input in the coil. These simulations have been performed at different frequencies of input voltage. But while plotting each graph, the frequency of input voltage has been kept constant. It can be observed from the figure that the variation of the magnetic flux density is more pronounced when the frequency of input voltage is 100 Hz. This variation starts becoming negligible as the frequency of the input voltage is increases.

Table 2-4 shows the numerical data of the current, voltage, power and resistance of the coil at different input voltage of the coil. It can be observed from this table that the power and the current in the coil are excessively high in order to produce 1 T magnetic field. Due to the thermal effects of such high value of electromagnetic field, the coil will be heated to excessively high temperature. This once again highlights the limitation of this study. This study is only meant as a proof-of-concept study and should not be taken as an actual representation of the MST coils.

2.4 Other Configurations

The coils used in MST can be of other configurations such as the cap, double stack and multi-stack coils. Figure 2-13 shows the screen shots of the different pattern of the coils. These screen shots have been taken from the graphics interface of the COMSOL software. Figures 2-14, 2-15, respectively, show the screen shots of the simulation of MST using the cap and the multi-stack coils.

It is worth noting that the simulation is carried out for an input voltage of 50V for cap coil, and 10V for the multi-stack coil. During the simulation, care has taken to obtain the magnetic field density of approximately 1 (unity) Tesla. If we keep the input voltage given to the coil constant at 50V, the magnitude of the magnetic field density produced by the coil increases beyond the acceptable limit. Hence the second configuration of the coil has been stimulated by a lower voltage. Simulations for a third configuration (double stack) as shown in Figure 13(c) have also been performed. This configuration turned out to be least effective and for the trials the input voltage has been set to 35V.

Voltage (V)	Magnetic Flux Density (T)
10	0.21
20	0.43
30	0.64
40	0.85
50	1.07

Voltage Value of 10
The following A,V,W, and Ohms Values

Derived Values Table	Values	Magnitude
Current (A)	84.0088-599.7825i	605.6373
Voltage (V)	9.9999-8.5695e-16i	9.9999
Power (W)	420.0439	
Resistance (Ohms)	0.00229	

Voltage Value of 20
The following A,V,W, and Ohms Values

Derived Values Table	Values	Magnitude
Current (A)	168.01757-1199.5649i	1211.2745
Voltage (V)	20.0+2.8033e-15i	20
Power (W)	1680.1757	
Resistance (Ohms)	0.00229	

Voltage Value of 30
The following A,V,W, and Ohms Values

Derived Values Table	Values	Magnitude
Current (A)	252.0264-1799.3475i	1816.9119
Voltage (V)	30.0-5.1487e-15i	30
Power (W)	3780.3953	
Resistance (Ohms)	0.00229	

Voltage Value of 40
The following A,V,W, and Ohms Values

Derived Values Table	Values	Magnitude
Current (A)	336.0351-2399.1210i	2426.8835
Voltage (V)	39.9999-1.4502e-15i	39.9999
Power (W)	6720.7028	
Resistance (Ohms)	0.00229	

Voltage Value of 50
The following A,V,W, and Ohms Values

Derived Values Table	Values	Magnitude
Current (A)	420.0439-2998.9125i	3028.1864
Voltage (V)	49.9999-5.5511e-16i	49.9999
Power (W)	10501.0981	
Resistance (Ohms)	0.00229	

Table2-4: Series of tables illustrating the current, voltage, power, and resistance, for varying voltage value at a constant frequency of 100 Hz.

(a) (b) (c)
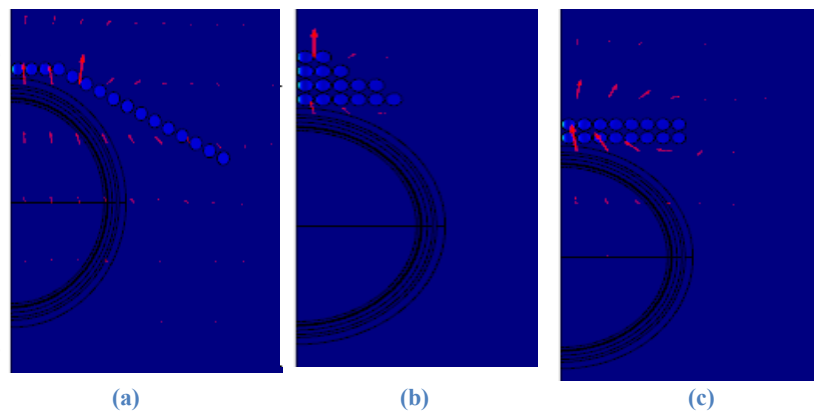
Figure 2-13: Axis-symmetric view of different configurations of electromagnetic coils: (a) cap, (b) multi-stack and (c) double stack coil.
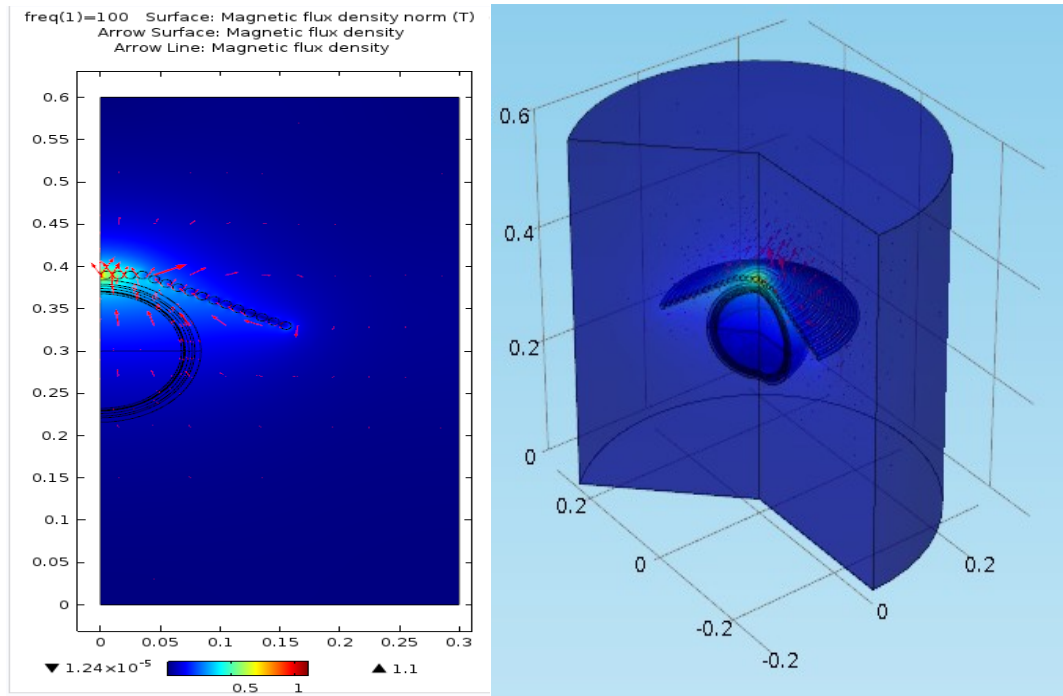
Figure 2-14: Axis-symmetric Magnetic Flux Density plot of MST using the cap coil, at 50 V.
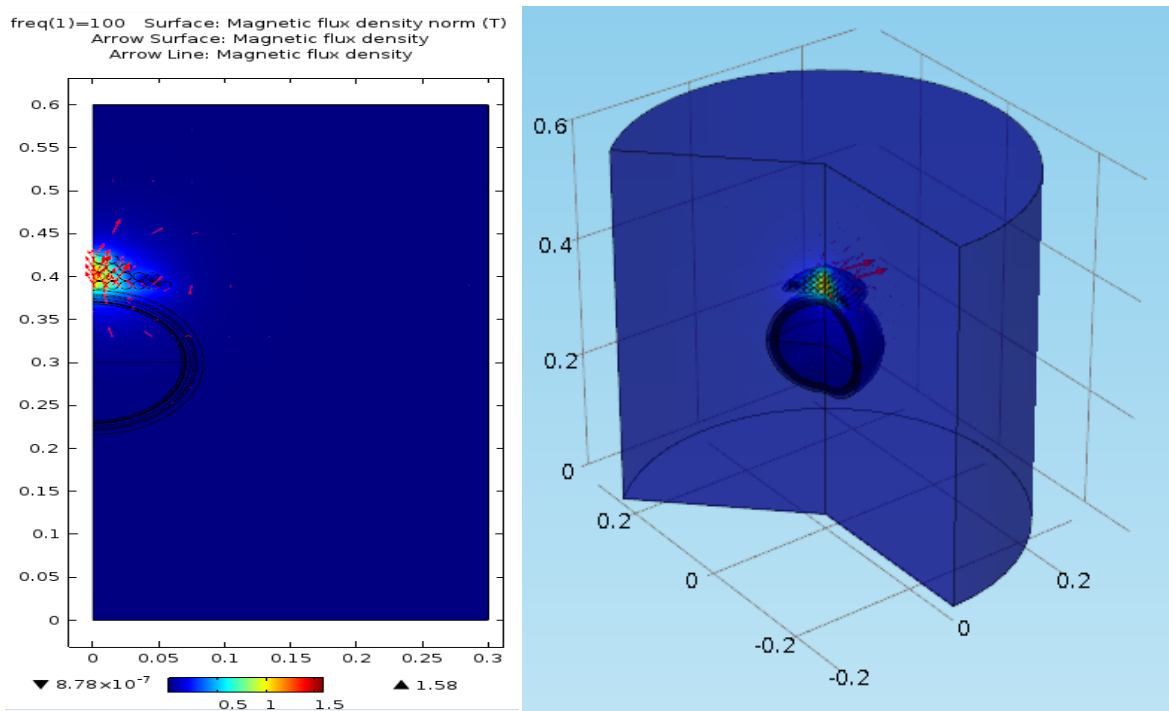
Figure 2-15: Axis-symmetric Magnetic Flux Density plot of MST using the multi-stacked coil, at 10 V.

Layer	Location	Current Density (A/m^2)	Current In that area (A)
Scalp	1	1.629	0.0373041
	2	1.584	0.0362736
	3	1.542	0.0353118
	4	1.518	0.0347622
	5	1.5069	0.03450801
Skull	7	3.71E-02	0.00084959
	8	3.66E-02	0.00083814
	9	3.66E-02	0.00083814
	10	3.64E-02	0.00083356
	11	3.61E-02	0.00082669
Cerebrospinal Fluid	13	7.336	0.1679944
	14	7.454	0.1706966
	15	7.544	0.1727576
	16	7.684	0.1759636
	17	7.7177	0.17673533
Gray Matter	19	1.273	0.0291517
	20	1.279	0.0292891
	21	1.295	0.0296555
	22	1.311	0.0300219
	23	1.339	0.0306631
White Matter	25	0.5083	0.01164007
	26	0.5144	0.01177976
	27	0.5209	0.01192861
	28	0.5274	0.01207746
	29	0.5367	0.01229043

Figure 2-16: Axis-symmetric model of the location (highlighted in lime green) where the data was sampled for the five different layers.

Figure 2-17 shows the data recorded given in the figure 16 in a graphical manner.
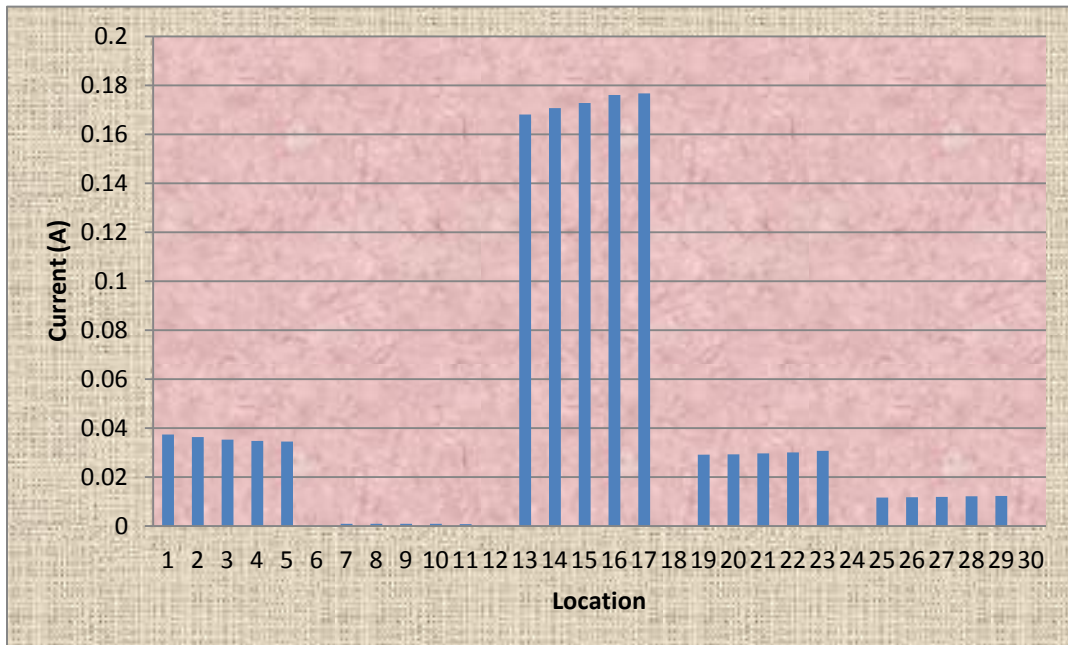
Figure 2-17: Graph illustrating the varying current within different layers of the brain, and sampled at the location shown in figure 17.

28

Figure 2-16 shows the data recorded at the 45° orientation of the cap coil. It can be observed that the maximum value of the induced current in the cerebrospinal fluid is around 175mA. The maximum value of the induced current by the single layer circular coil was around 128mA. Thus it can be observed that the performance of the cap coil is better than the single layer circular coil. A detailed comparison of the all the types of coils will be performed in the last section of this chapter. But this is just a brief but important observation.

Figure 2-18 shows the simulation data for the multi-stacked coil. In this case, the input voltage to the coil is 10V in order to produce a magnetic field density comparable to a practical MST device. Figure 2-19 describes the data in the graphical manner. It can be seen from these two figures that the maximum value of current induced is around 176mA which is comparable to the current induced by the cap coil. But the same value of current is induced at a much lesser input voltage. It can be inferred from this that the performance of the multi-stacked coil is much better than the cap coil and the stacked coil because it gives almost the highest value of induced current at the lowest input power.

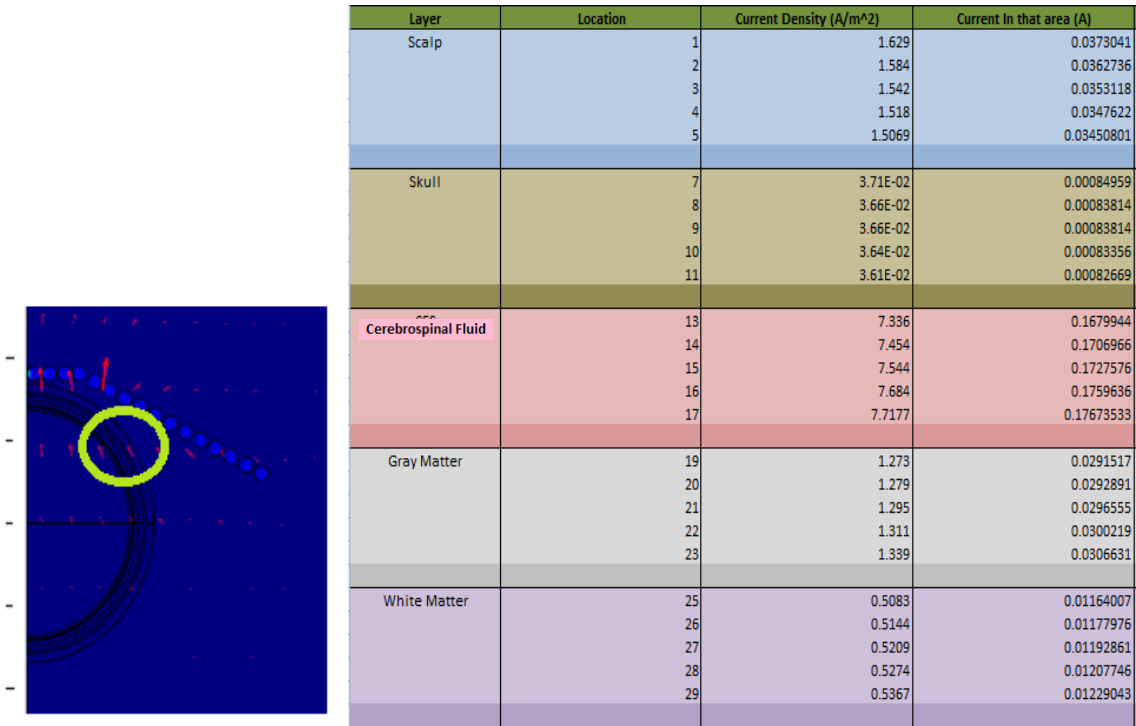| Layer	Location	Current Density (A/m^2)	Current In that area (A)
Scalp	1	0.1103	0.00252587
	2	0.2044	0.00468076
	3	0.3079	0.00705091
	4	0.2089	0.00478381
	5	0.08369	0.001916501
Skull	7	8.19E-03	0.000187551
	8	8.21E-03	0.000188009
	9	8.21E-03	0.000188009
	10	8.13E-03	0.000186177
	11	8.05E-03	0.000184345
Cerebrospinal Fluid	13	1.7909	0.04101161
	14	1.73	0.039617
	15	7.695	0.1762155
	16	1.677	0.0384033
	17	1.652	0.0378308
Gray Matter	19	0.3163	0.00724327
	20	0.3141	0.00719289
	21	0.3103	0.00710587
	22	0.3071	0.00703259
	23	0.2455	0.00562195
			0
White Matter	25	0.129	0.0029541
	26	0.129	0.0029541
	27	0.127	0.0029083
	28	0.126	0.0028854
	29	0.123	0.0028167

Figure 2-18: Axis-symmetric Model of the location (highlighted in lime green) where the data was sampled for the five different layers.
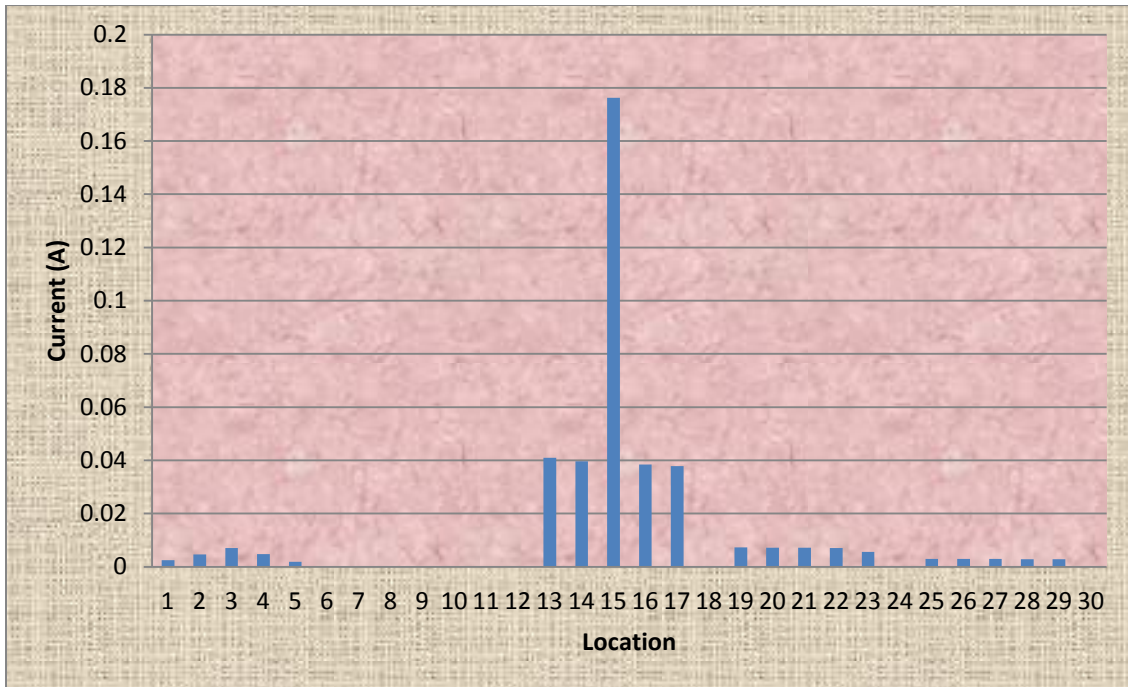
Figure 2-19: Graph illustrating the varying current within different layers of the brain, and sampled at the location shown in figure 32.

As mentioned earlier in the present section, a fourth configuration, namely double stack coil has also been considered. Like in the previous cases, the input voltage was reduced so that a reasonable induced current can be achieved while maintaining a magnetic field density of about 1 Tesla. However, at this magnetic field density, the coil gave relatively low induced current. Hence to push the coil's ability to produce a maximum realistic coil magnetic field of about 2 Tesla and for achieving a reasonable induced current of about 100mA, the voltage was set to 35 V. The results of this case have been presented only for illustrative purposes.

2.5. Coil comparison results and discussion

Table 2-5 shows the comparison of the performance of the single, cap and multi-stack coils, considering the maximum induced current in the Cerebrospinal fluid. The data predicted above shows that maximum current is induced in the Cerebrospinal fluid region when compared with maximum induced currents in other regions. Hence, this current magnitude has been chosen for meaningful comparison of performance and to arrive at appropriate conclusions.

30

It can be observed that from the table that the multi-stacked coil gives the maximum value of induced current in the brain with the least input voltage required by the device. This is definitely an optimum performance and thus it can be concluded that the multi-stacked coil can be considered as the most preferred coil configuration amongst the coil types studied. Further, as discussed in the previous section, the double-stack configuration appears to be the least effective amongst the other configurations investigated in the present research.

Type of coil	Input voltage to the coil (V)	Maximum induced current (mA) in the cerebrospinal fluid
Single layer circular coil	50	128
Cap coil	50	175
Multi-stack coil	10	176
Double stack coil	35	110

Table 2-5: Comparison of the maximum induced current and the input voltage of the coil for different types of the coils.

Another consistent observation that has already been mentioned in the previous sections is that the current induced is the maximum in the cerebrospinal fluid and not in the gray matter. However, from the psychiatric perspective, activating the neurons of the gray matter is more important than inducing current in the cerebrospinal fluid. But, the simulations indicate that this fluid acts as a major barrier in inducing current in the gray matter and warrant further research in the MST device in order improve efficient induction of current in the gray matter.

There is one limitation of this study that needs to be mentioned over here. The coils have been modeled as a simple electromagnet in this study. But in reality, the technology of functioning of this coil is far more complex and can be known only from the manufacturer's data, X-rays and impedance measurements of the coils. Hence this is only a proof-of-concept study. But still it is relevant because the effect of the magnitude of magnetic field density of around 1 Tesla on the brain has been investigated.

2.6 Closure

In this way the virtual simulation of the MST procedure has been performed using the COMSOL software by modeling the human brain by a sphere. The performance of the single layer coil has been investigated and documented in detail in this thesis. It has been found out that the probing at 45° orientation yielded the best values of induced current in the brain. After that data for other configurations, namely, cap and multi-stack coil has been documented only at this orientation although the simulations have been performed at other orientations also. These extra simulations also yield the same fact that the 45° orientation gives the maximum values of induced current. Due to this these simulations have not been presented in the thesis report. The input voltage to the coil has been kept such that a maximum value of magnetic field density is around 1 Tesla is obtained. The reason behind this is that once we have the relevant conclusion for a magnetic field density of 1 Tesla, we can confidently predict the performance of the device for an increased magnetic field density. Our analysis concluded that the multi-stack coil showed the best performance and the double stack coil has been the poorest amongst all the configurations of the coils.

Chapter 3 Mathematical Modeling of Neuron Spiking and Threshold Adaptation

3.1 Introduction

This chapter starts with the description of the anatomy and physiology of the neuron for the purposes of gaining an understanding of the underlying mechanics of neuron spiking. This would also aid in understanding of a suitable mathematical model that describes the dynamics of neuron spiking. It is known that the neuron spiking mechanism is instrumental in transmitting information in the form of electrical impulses.

The functioning of the different types of channels such as the ligand gated channels and voltage gated channels is discussed. The neuron chemistry is explained in detail in order to understand the concept of action potential and transmission of electrical impulse through the neuron. Some of the topics of the neurons chemistry introduced in this section are ionic diffusion, sodium potassium pump and resting membrane potential. This discussion is followed by the main topic of the neuron physiology, that is, action potential or transmission of electrical impulse through the neuron. The sequences of changes that occur in the neuron after a neurotransmitter molecule gets embedded on the ligand gated channel are described. Once the ligand gated channels open, there is a change in the membrane potential of the neuron and this causes the voltage gated sodium and potassium channels to open. The conductance of the voltage gated sodium and potassium channels is such that the sodium channels open first and close rapidly, while there is a lag in opening and closing of the potassium channels. The details of how very few ions of sodium and potassium cause a change in potential in the neuron have been explained in this chapter.

The second part of the chapter introduces a mathematical model which predicts the spiking of the neurons when subjected to random input current. This model consists of three coupled first order non-linear differential equations. Three different cases, each having a particular behaviour of steady state threshold potential, have been numerically simulated via Simulink. It has been

shown that the Cases 2 and 3 demonstrate the threshold adaptation associated with neuron spiking which is not seen in Case 1 . The simulation results give a very vivid explanation of the threshold dynamics which is the main topic of the second part of this thesis.

3.2 Theory of transmission of electrical impulse via neurons
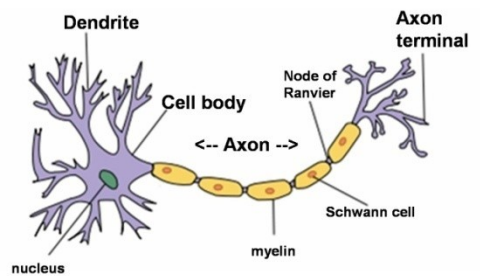
3.2.1 Concept of neuron activation:

Figure 3-1 Neuron

Ref: Chapter 12 NEURONS. (n.d.). Retrieved May 11, 2015, from
http://users.tamuk.edu/kfjab02/Biology/AnimalPhysiology/B3408 Systems/BIOL 3408 Chapter 11 Neurons.htm

Neurons are used to process information in the brain and are responsible for all the activities of the central and peripheral nervous system. Neurons can have varying length from a fraction of millimeters in the brain and up to a meter in the spinal cord. Also, they have different firing rates ranging up to 1000 impulses per second and different velocities ranging from 0.2 to 120 m/s.

The neuron consists of dendrites, soma (body) where the nucleus of the neuron is located, axon, Schwann cells which have the coating of myelin sheath, node of Ranvier and axon terminal. The ligand gated channels which are part of the dendrites are shown in Figure 3-3 and the the Voltage gated channels which lie along the axon are shown in Figure 3-4. These channels are instrumental for the occurrence of action potential which is also called neuron spiking. The ligand gated channels initiate the process of action potential while the voltage gated channels sustain it.
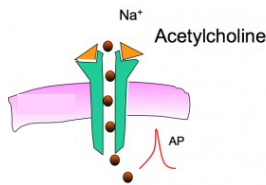
Ligand-gated channel

Figure 3-4 Ligand gated channel

Ref: Excitability and Membrane Electropotential. (n.d.). Retrieved February 11, 2015, from
http://webanatomy.net/237/channels/channels.htm
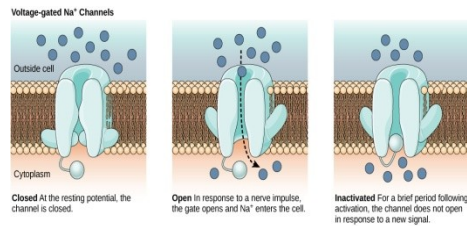
Figure 3-5 Voltage gated Na channels

Ref: Nerve Impulse Transmission within a Neuron: Resting Potential - Boundless Open Textbook. (n.d.). Retrieved May 11, 2015, from https://www.boundless.com/biology/textbooks/boundless-biology-textbook/the-nervous-system-35/how-neurons-communicate-200/nerve-impulse-transmission-within-a-neuron-resting-potential-761-11994/

Figure 3-6 Voltage gated K channels

Ref: Voltage gated potassium channels. (n.d.). Retrieved May 11, 2015, from
https://www.studyblue.com/notes/note/n/chapter-4-neuronal-physiology/deck/722174

Chemicals called as neurotransmitters (Acetylcholine) released by the neuron get attached to the dendrites when an electric impulse needs to be transmitted by the neuron. These open the ligand gated channels and sodium ions rush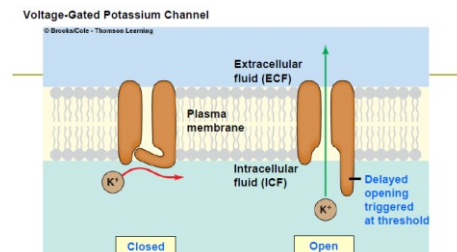 into the body of the neuron and increase its potential. When the potential in the body of the neuron reaches the threshold potential, the membrane potential undergoes a sudden and reversible change referred as the action potential which opens the voltage gated sodium and potassium channels due to which the electric impulse is transmitted along the axon. This phenomenon of action potential and transmission of impulse through the neuron will be explained in detail in the forthcoming sections.

3.2.2 Ionic diffusion and resting membrane potential

A brief explanation about the Potential build-up across a membrane is provided first so that the chemistry behind the process can be understood. Figure 3-5a show a Membrane having a concentrated salt solution on one side 2 and a less concentred salt solution (with respect to the side 2) on side 1. Due to the chemical gradient, cations (+ ve ions) and anions (- ve ions) will start diffusing across the membrane. If due to some reasons, the permeability of cations is more than that of the anions, they will propagate more rapidly across the membrane and a negative potential with respect to the reference electrode (ground) will be set up across the membrane as shown in the figure 3-5b. This is basically due to different amount of diffusion rates and is one of the main reasons of development of resting membrane potential in the neuron.
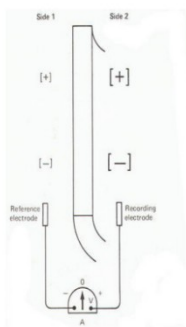

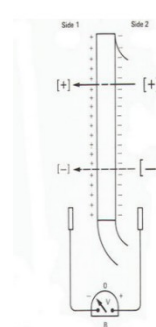**Figure 3-7a) Membrane showing no potential**   **Figure 3-5b) Membrane showing potential**

Ref: MEMBRANE POTENTIALS. (n.d.). Retrieved May 11, 2015, from
http://www.humanneurophysiology.com/membranepotentials.htm

36

3.2.3 Concept of electrochemical equilibrium
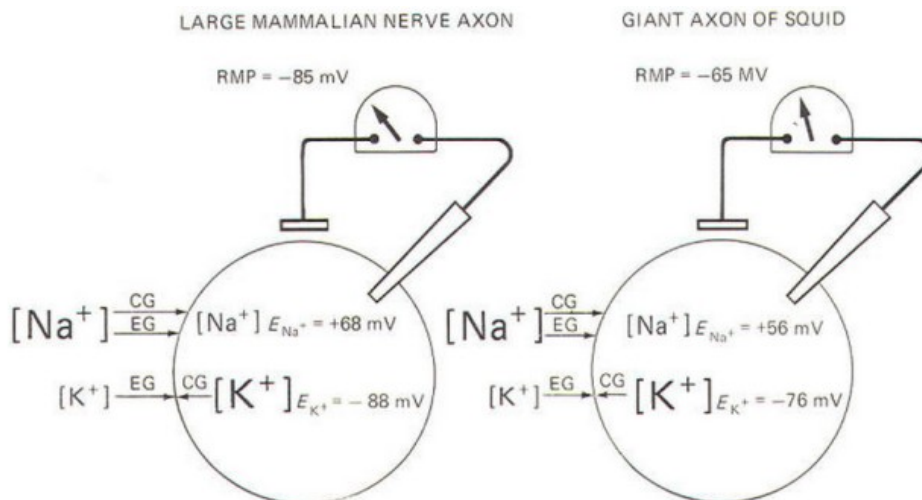
Figure 3-8 Electrochemical equilibrium

Ref: MEMBRANE POTENTIALS. (n.d.). Retrieved May 11, 2015, from
http://www.humanneurophysiology.com/membranepotentials.htm

The potential maintained during the resting phase of the neuron is called the resting membrane potential. The concept of electrochemical equilibrium is very important to understand how the membrane potential is kept at a particular value during the steady state, i.e. when it does not transmit any impulse. First consider that there are only potassium ions in the neuron and the concentration of potassium ions is more in the interior of the neuron than the exterior. Due to the chemical gradient, potassium ions will try to diffuse to the outside of the membrane. As these ions start diffusing through the membrane, a positive charge will be built across the membrane as illustrated previously in Figure 3-5b. During this process, a stage is reached when the electric gradient developed due to the diffusion of ions becomes equal to the chemical gradient and this stops further diffusion of the ions across the membrane and the potassium ions are considered to be in electrochemical equilibrium. It can be shown that the electrochemical equilibrium of potassium ions is -88 mV in large mammalian nerve axon and -76 mV in the giant axon of a squid.

3.2.4 Resting membrane potential.
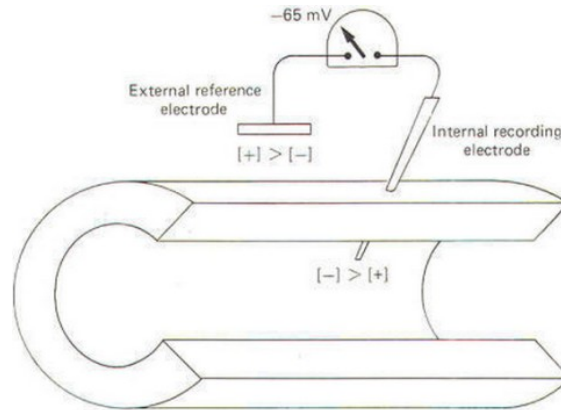
Figure 3-9 Resting membrane potential

Ref: MEMBRANE POTENTIALS. (n.d.). Retrieved May 11, 2015, from

http://www.humanneurophysiology.com/membranepotentials.htm

It has been experimentally observed that the intracellular potential of the axon is always negative with respect to extracellular potential (considered as Reference or ground) as illustrated in Figure 3-7. This potential is -85 mV in mammalian axon and -65 mV in the giant axon of the squid. All cells of the different organs of the body have some resting membrane potential. However, the cells of muscles and nerves are the only ones whose resting membrane potential can be altered.

3.2.5 Ionic imbalance of sodium and potassium.

Figure 3-10 Sodium and potassium pump

Ref: MEMBRANE POTENTIALS. (n.d.). Retrieved May 11, 2015, from

http://www.humanneurophysiology.com/membranepotentials.htm

38

Electrochemical equilibrium does not exist for the sodium and the potassium ions in the axon. Sodium ions constantly try to diffuse towards the interior of the membrane due to their higher (+ ve) electrochemical equilibrium potential than the resting membrane pote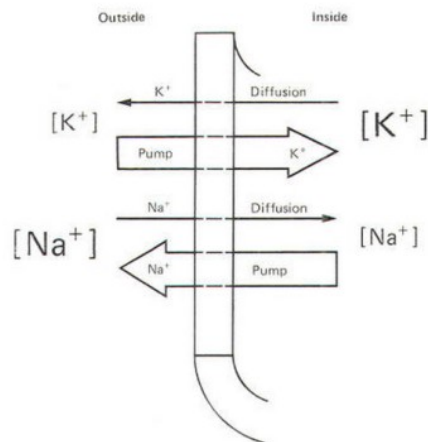ntial (-ve). Similarly, the potassium ions try to move outwards and there is constant diffusion of ions across the membrane. If there is constant diffusion of ions across the membrane, the question arises about how the resting membrane is maintained in the neuron. The answer to this question is given by the existence of sodium-potassium pump. This is shown in figure 3-8. This pump is an active transport system of ions opposite to their diffusion pathways. This pump balances the lack of electrochemical equilibrium of the sodium and potassium ions and maintains the resting membrane potential of the neuron at a constant value.

3.2.6 Action potential

Figure 3-9 shows how the changes that occur in the membrane potential when the action potential is initiated in the neuron. When the neurotransmitter molecules get embedded on the ligand gated channels of the dendrites of the neuron, these channels open and sodium ions rush into the body of the neuron. This causes the membrane potential of the neuron to increase. If the membrane potential crosses the threshold potential, there is a sudden increase of the membrane potential and it attains a positive value. This happens due to the opening of the voltage gated sodium channels. The sodium channels close rapidly after opening. Due to this, the membrane potential reaches its maximum value and it starts to decline when the sodium channels start closing. The voltage gated potassium channels open at this stage and further cause the membrane potential to become negative. Some hyper-polarization occurs due to this which is rectified by Sodium-Potassium pump and the membrane potential comes back to the resting potential.
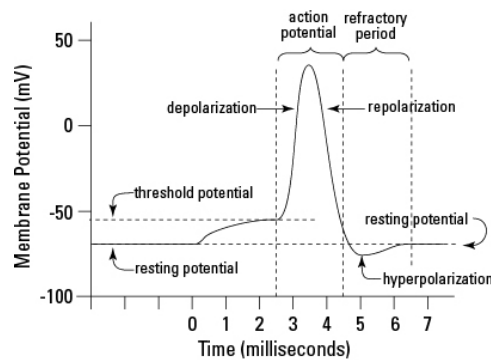

Figure 3-11 Action potential

39

3.2.7 Nerve impulse transmission

This section deals with the transmission of electrical impulse through the axon of the neuron. Figure 3-10 shows the time capture of the signals passing through an axon displayed as *t=1, t=2* and *t=3*. It consists of the body of neuron to its left and the axon terminal to its right described previously in Figure 1. In this diagram, the impulse is considered to represent signals travelling from left to right. Once the potential at the left end of the axon crosses the threshold voltage, the voltage gated sodium channels at that site open and there is a sudden influx of sodium ions at that site. This causes the membrane potential to become positive at that site and action potential is initiated at that site. Once the active current pierces the membrane, some of it passes to the next site of the axon which is to its right. This small portion of the active current which passes to the next site of the axon is called the passive current. The passive current passes only to the right of the axon because the voltage gated sodium channels to its left close within a fraction of second after opening. This passive current is sufficient to cross the threshold potential of the neuron at this site and this result in an action potential at the next site of the axon. The impulse travels along the neuron in this manner.

As mentioned earlier, the voltage gated sodium channels close within a fraction of second after their opening. After that the voltage gated potassium channels open and the potassium ions rush outside in order to make the voltage across the membrane negative. This results in making the potential at that site back to negative. It requires a very few ions to cause these potential changes at the site of the axon. The balance of the sodium and potassium ions is restored back by the sodium-potassium pump, whose function has been explained in section 3.2.5.
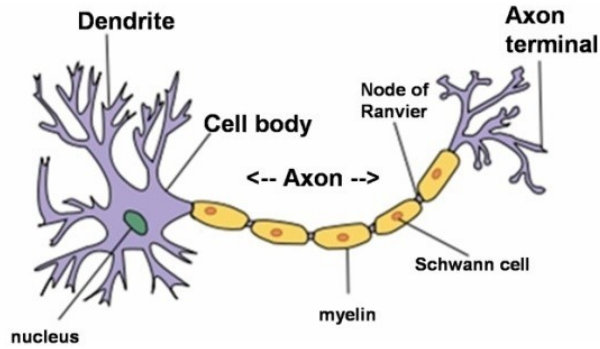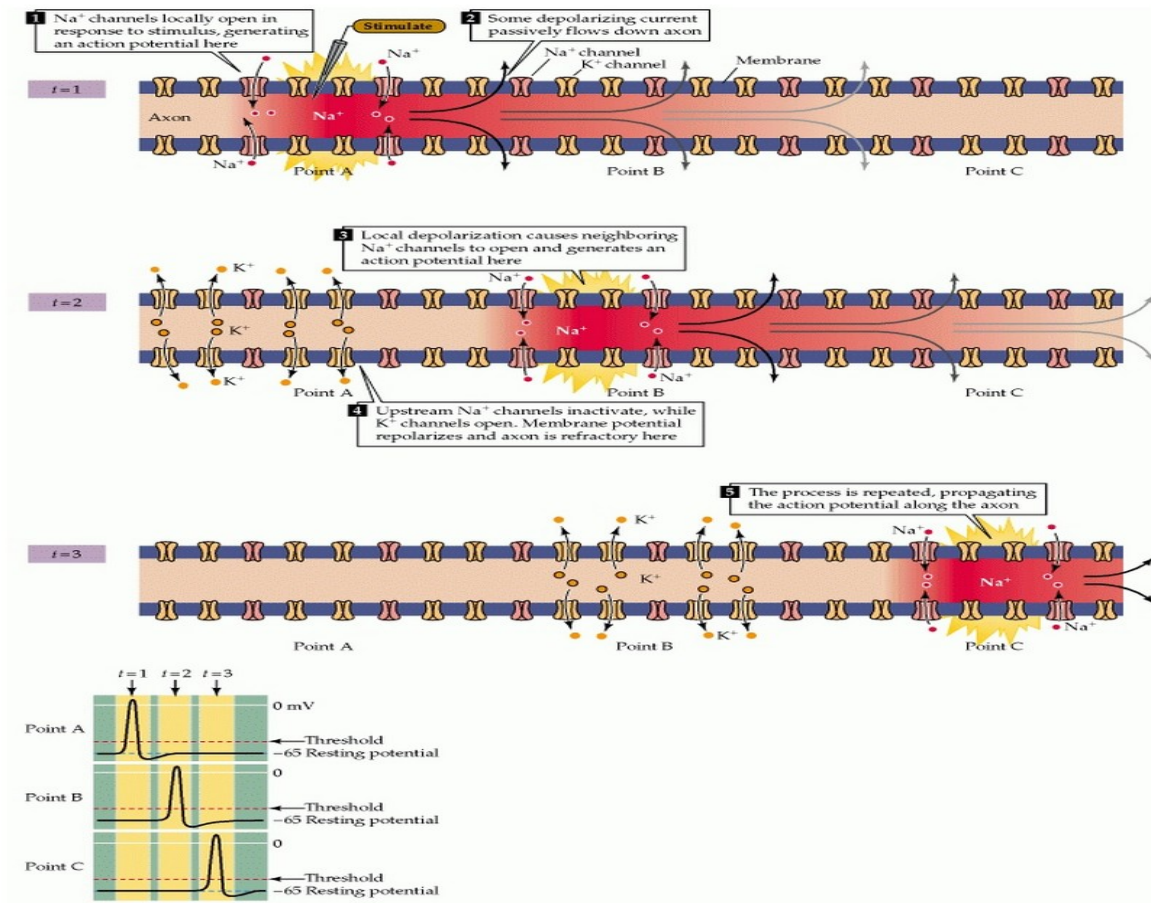
Figure 3-1 Neuron

Figure 3-12 Active and passive currents

Ref: Purves, D. (n.d.). Long-Distance Signaling by Means of Action Potentials. Retrieved May 11, 2015, from http://www.ncbi.nlm.nih.gov/books/NBK11107/

3.3 Proposed mathematical model for simulation of neuron spiking

3.3.1 Basis of Proposed Mathematical Model

The mathematical model used in the present research has been cited from a paper written by (Bertrand Fontaine, Jose´ Luis Pen˜ a1, Romain Brette). These researchers have performed experiments on a barn owl and fitted the data obtained from their experiments by a deterministic mathematical model.

In their experiments, the researchers have used earphones in order to transmit a white noise filtered between 0.5 to 10 kHz frequencies to the ears of the owl. They measured the membrane potential (V_m) of the sensory nerves of the owl and recorded when the neurons were spiking. They observed that low frequency noise input is filtered out by the neuron because the threshold voltage of the neuron also increases when a low frequency signal is given to the neuron. As the membrane potential never crosses the threshold potential, the neuron does not spike for input signal of low frequencies.

The researchers then tried to mathematically predict this spiking of neurons and came up with a deterministic mathematical model, which will be described in detail in the next section. They found out that this model could predict the spiking of the neurons with an accuracy of 89%.

3.3.2 Mathematical Model for Threshold Adaptation

The mathematical model used by the above mentioned researchers can be described by the following first order coupled non-linear differential equations. They are as follows:

$$\tau_\theta \frac{d\theta}{dt} = \theta_\infty(V_m) - \theta \,, \qquad \text{3-1}$$

where

τ_θ = time constant,

$\theta_\infty(V_m)$ = steady state threshold,

V_m = membrane potential,

θ = threshold potential.

and

$$\theta_\infty(V_m) = \alpha(V_m - V_i) + V_T + k_a \log\left(1 + \exp\left(\frac{V_m - V_i}{k_i}\right)\right) \quad .$$

3-2

In Equation 3-2,

V_i = critical voltage, below and above which $\theta_\infty(V_m)$ is described by a smooth function with different slopes,

V_T = minimum threshold voltage,

and α, k_a, k_i are parameters which are used to plot the curve of $\theta_\infty(V_m)$ vs V_m.

$$\tau_m \frac{dV_m}{dt} = (E_L - V_m) + \Delta\exp\left(\frac{V_m - \theta}{\Delta}\right) + (R_m)I \quad ,$$

3-3

where

E_L = Reverse potential of the leak current,

Δ Characterises the sharpness of initiation,

R_m = membrane resistance,

I = Input current.

Three different simulations have been performed during this study. They vary according to the nature of the graph of steady state threshold value voltage vs. membrane potential.

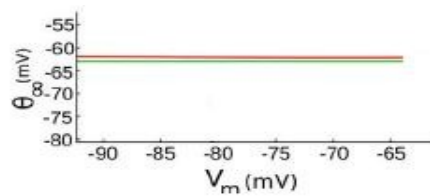**Case 1:** Constant steady state threshold values with respect to the membrane potential:

Figure 3-13 Graph of steady state threshold vs. membrane potential

The values of different constants used in the equations are given in a tabular manner as follows:

Parameters and/or constants	Values
α	0
k_a	0 mV

V_T	-63 mV
V_i	-67 mV
τ_θ	5 ms
τ_m	5 ms
E_L	-70 mV
Δ	1 mV
R_m	100 MΩ
I	Mean = 71×10^{-12} A Variance = 1.6×10^{-19} (A)^2

Table 3-4 Table of different values of constants for Case 1

Case 2: Rectified steady state threshold values with respect to the membrane potential:

Figure 3-14 Graph of rectified steady state threshold vs. membrane potential

The values of different constants used in the equations are same as given in the table mentioned above with the following exceptions:

Parameters and/or constants	Values
k_a	5mV
k_i	10 mV
I	Mean = 71×10^{-12} A Variance = 5×10^{-18} (A)^2

Table 3-5 Table of different values of constants for Case 2

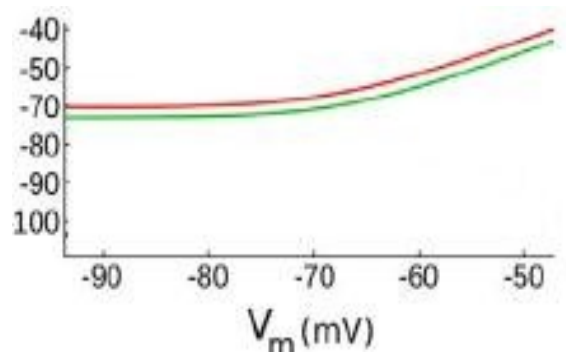**Case 3:** Linear steady state threshold values with respect to the membrane potential:
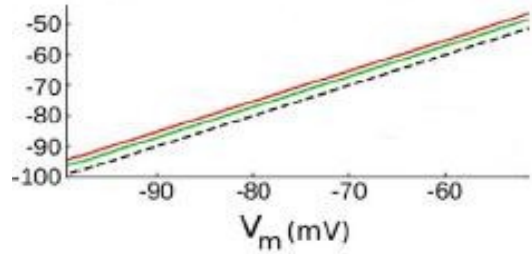
Figure 3-15 Graph of linear steady state threshold vs. membrane potential

The values of different constants used in the equations are given in a tabular manner as follows:

Parameters and/or constants	Values
α	1
k_a	0 mV
V_T	-63 mV
V_i	-66 mV
τ_θ	3 ms
τ_m	5 ms
E_L	-70 mV
Δ	1 mV
R_m	100 MΩ
I	Mean $= 71 \times 10^{-12}$ A Variance $= 3 \times 10^{-18}$ (A)^2

Table 3-6 Table of different values of constants for Case 3

3.3.3 Simulation results

The next step in this study was to perform numerical simulations based on the mathematical model presented in section 3.3.2 considering the above mentioned three cases. The simulation was performed in the MATLAB/Simulink environment and the graphs have plotted using Matlab. Each case was simulated for 2 seconds. The solver used for the simulation was ode45 (Dormand-Prince) with a variable step. The random number block in Simulink was used to give the random input current to the model. The threshold potential adaptation (variation of θ) was

observed in the second and third cases This phenomenon is explained in detail with the help of graphs as follows:
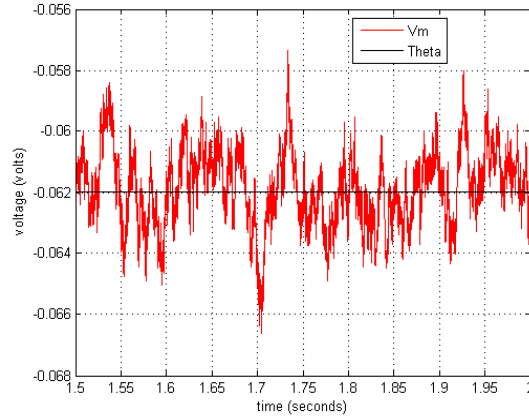
Figure 3-16 Graph of V_m and Theta (θ) vs. time
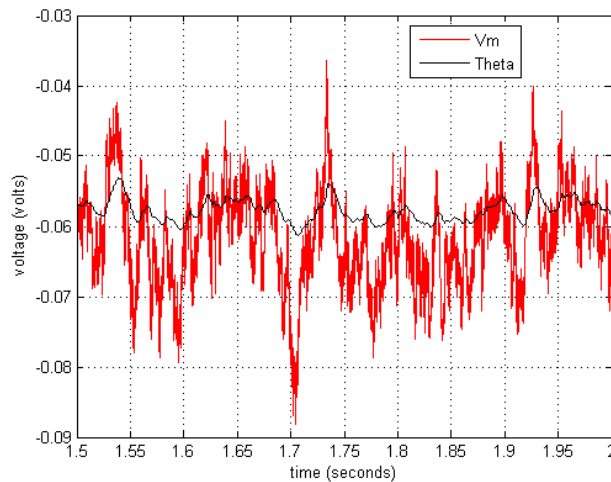
Figure 3-17 Graph of V_m and Theta (θ) vs. time

Case 1: Constant steady state threshold values with respect to the membrane potential:

Figure 3-14 shows the graph of V_m and θ vs. time. This is the response of the neuron for the random input current given to it. When θ has a constant value, the neuron spikes for any frequency of the random noise. Adaptation of the neuron is not seen in this case and threshold dynamics does not come into play.

Case 2: Rectified steady state threshold values with respect to the membrane potential:

Figure 3-15 shows the graph of V_m and θ vs. time for the second case. It can be clearly seen in this graph that θ varies with respect to time and it adapts to the membrane potential. Whet the membrane potential increases, the threshold potential also increases and tries to prevent the spiking of the neuron. But if the increase in membrane potential is fast enough, the threshold potential cannot increase with this proportion. In this case the value of membrane potential crosses the threshold potential and the neuron spikes. In this way, the neuron acts as a filter and eliminates the low frequency signals given to it. Although we do not come to know which frequency is eliminated from the graph, this pattern and concept is clearly demonstrated from it.

Case 3: Linear steady state threshold values with respect to the membrane potential:
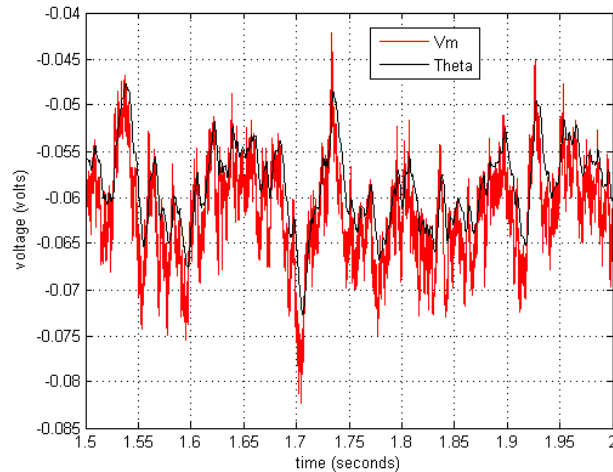
Figure 3-18 Graph of V_m and Theta (θ) vs. time

Figure 3-16 shows the graphs of V_m and θ vs. time for the third case. Threshold adaptation dynamics similar what was described in Case 2 is also observed in this case and the neuron spikes filters the lower frequencies and spikes only for higher frequency current inputs.

3.3.4 Relationship between neuron spiking and MST procedure simulation

During the finite element analysis of the brain model during the MST procedure, the maximum current induced in the brain was determined. Ideally, the present study intended to input this current into a mathematical model describing the functioning of the human neuron. The neuron mathematical model would then be simulated using Matlab and Simulink and more

comprehensive investigations of the neuron spiking could be performed. But within the allotted time frame, the present study was limited to the response of sensory nerves of a barn owl when subjected to a random input current. However, it has been proposed in this thesis that when the barn owl study is extended to the neuron spiking in humans or from other models available within the mathematical neuroscience community, such a linkage of psychiatry and theoretical neuroscience could be carried out in the future and its results can be verified by psychiatrists.

3.4 Closure

This chapter deals with the mathematical modeling of the neuron. In order to understand this, the neuron anatomy and physiology has been discussed before introducing the model. Special emphasis has been given to explain the concept of action potential and nerve impulse transmission. The mathematical model which describes the neuron spiking of a barn owl has been selected for simulation purposes. The simulations, which have been carried out using Matlab and Simulink, demonstrate the concept of threshold adaptation of the neurons. This adaptation is observed when the steady state potential is rectified or linear. The last part of this chapter hints that how this concept of theoretical neuroscience can be improved, by incorporating a model of a human neuron, in order to completely replicate the MST procedure.

Chapter 4 Conclusions and Recommendations

This thesis consists of the study of MST and the mathematical modeling of the neuron. In order to achieve the proposed goals of this study, the anatomy and physiology of the brain and the neuron has been studied. It has been found out that the prefrontal cortex region is less active with patients suffering from major depression. The neurons of this region of the brain have to be activated in patients suffering from treatment resistant depression. ECT has been the choice for this purpose used by the psychiatrists until now. But it has a serious side effect of memory loss. MST has been developed in order to have the same positive effects of ECT with minimum memory loss.

A literature review has been conducted to find out the merits and de-merits of MST. Although MST might have some limitations, its advantages outweigh the limitations and hence it has been observed that it is worth doing the computational study of MST.

The scope and objective of the thesis is defined after the literature review and it is to virtually simulate the MST procedure and show the effect of the current induced in the brain on the spiking of the neuron. In this way the thesis is divided into two broad parts. The first one is the FEA of the human brain and the second is the mathematical of the neuron.

After completing all these prerequisites, FEA of the human brain is carried out using the COMSOL software. The head has been modeled as a sphere having concentric layers corresponding to the different tissues of the brain. Relevant conductivity properties have been assigned to each layer of the sphere. After some simulations, the geometry of the coil has been found out in order to produce a magnetic field density of approximately 1 Tesla. The input voltage to the coil and its frequency has been set as 50 V and 100 Hz respectively.

Further simulations reveal that the maximum current induced in the brain is in the cerebrospinal fluid and its maximum value is probed at an orientation of 45° with respect to the vertical axis.

Its value is 128 mA for a single layer coil. It has been observed that magnetic field density drastically reduces as the frequency of excitation of the coil is increased when the voltage applied to the coil is kept constant. Another observation is that the variation of magnetic field density with respect to input voltage, when the frequency of excitation is kept constant, is most prominent when the frequency has the lowest value of 100Hz.

The next part of FEA consists of studying the performance of different configurations of the coil such as the cap coil, double stacked coil and the multi-stacked coil. It has been found out that the multi-stacked coil is the most effective and the double stacked coil is the least effective coil configuration.

The second broader part of the project consists of find a suitable mathematical model of neuron spiking. But before that the concept of neuron spiking has been understood by studying the concept of action potential, nerve impulse transmission and related topics. A mathematical model describing the neuron spiking of the sensory nerves of the barn owl has been selected for simulation purposes. Simulink software has been used for the simulation and the concept of threshold adaptation has been studied and discussed in detail in this part of the thesis. It has been observed that the threshold adaptation exists when the steady state threshold potential is rectified or linear with respect to the membrane potential. Threshold adaptation is the change of threshold potential with respect to time.

It may be noted that this thesis consists of combination of psychiatry and theoretical neuroscience in order to understand MST and neuron spiking. Although the mathematical model the human neuron has not been simulated, the best possible work has been done within the given timeframe that was available for this study.

4.1 Thesis contributions:

- Created a head model suitable for FEA of brain using COMSOL software for simulation the MST procedure. The head model consists of a sphere consisting of concentric layers each representing a specific tissue in the brain. Appropriate conductivity properties are applied to each layer of the sphere.

- Determined the geometrical dimensions of the coil via trial simulations with the input voltage fixed to 50 V and its frequency equal to 100 Hz. The best probing results of the induced current was observed at 45° orientation with respect to vertical axis.

- Among the predicted current in the various layers considered, the largest induced current was found in the cerebrospinal fluid. Further, the cerebrospinal fluid was found to act as barrier in inducing current in the gray matter of the brain.

- Among the simulations carried out on different configurations of the coil, namely, cap coil, double stacked coil and multi-stacked coil, the multi-stacked coil was found to give the best performance while the double stacked coil was the least effective.

- Identified a suitable mathematical model in the form of three coupled non-linear differential equations, for describing the threshold dynamics of neuron spiking. This deterministic model was based on experimental recordings of neuron spiking when subjected to random noise.

- The model based numerical predictions confirmed the threshold adaptation for constant steady state potential, rectified steady state potential and linear steady state potential associated with neuron spiking.

4.2 Recommendations for Future Work

- Appropriate mathematical model the spiking of the human neuron should be developed with relevant parameters and a proper connection should be made between psychiatry and theoretical neuroscience. The results obtained from this work should be verified from psychiatrists.

- Other software which is used for simulation should be explored in order to build complex coil configurations. The capabilities of COMSOL could be enhanced by using its CAD import module.

- Based on the present analysis, the cerebrospinal fluid acts a barrier for induction of current in the gray matter. Hence, the technology of the MST device should be improved in order to induce more current in the gray matter.

- A patient-specific head model could be used for the MST simulations performed via COMSOL. This would result in increasing the accuracy and effectiveness of the simulation.

References

Deng, Z., Lisanby, S., & Peterchev, A. (2011, January 19). Electric field strength and focality in electroconvulsive therapy and magnetic seizure therapy: A finite element simulation study. Retrieved August 31, 2015.

Fontaine, B., Pen˜ a, J., & Brette, R. (2014, April 10). Spike-Threshold Adaptation Predicted by Membrane Potential Dynamics In Vivo. Retrieved August 31, 2015.

Havas, M. (2004). Biological Effects of Low Frequency Electromagnetic Fields. Retrieved August 31, 2015.

Human Physiology - Neurons & the Nervous System. (n.d.). Retrieved May 11, 2015, from http://people.eku.edu/ritchisong/301notes2.htm

Kayser, S., Bewernick, B., Grubert, C., Hadrysiewicz, B., Axmacher, N., & Schlaepfer, T. (2010, September 14). Antidepressant effects, of magnetic seizure therapy and electroconvulsive therapy, in treatment-resistant depression. Retrieved August 31, 2015.

Kirov, G., Ebmeier, K., Scott, A., Atkins, M., Khalid, N., Carrick, L., . . . Lisanby, S. (2008, August 1). Quick recovery of orientation after 100 Hz magnetic seizure therapy (MST) for major depressive disorder. Retrieved August 31, 2015.

Magnetic Seizure Therapy. (n.d.). Retrieved August 22, 2015, from http://www.magventure.com/en-gb/Researchers/Applications/Magnetic-Seizure-Therapy

MEMBRANE POTENTIALS. (n.d.). Retrieved May 11, 2015, from http://www.humanneurophysiology.com/membranepotentials.htm

Propagation of the Action Potential (Section 1, Chapter 3) Neuroscience Online: An Electronic Textbook for the Neurosciences | Department of Neurobiology and Anatomy - The University of

Texas Medical School at Houston. (n.d.). Retrieved May 11, 2015, from http://nba.uth.tmc.edu/neuroscience/m/s1/chapter03.html

Purves, D. (n.d.). Long-Distance Signaling by Means of Action Potentials. Retrieved August 31, 2015, from http://www.ncbi.nlm.nih.gov/books/NBK11107/

White, J., Rubinstein, J., & Kay, A. (2003). Channel noise in neurons. Retrieved August 31, 2015.

Curriculum Vitae

Name: Abhijeet Wadkar

Post-secondary   Vishwakarma Institute of Technology,
Education and   Pune, Maharashtra, India
Degrees: 1999-2004 B.E.

The University of Western Ontario
London, Ontario, Canada
2010-2012 M.Eng.

The University of Western Ontario
London, Ontario, Canada
2013-2015 MESc

Related Work   Teaching Assistant
Experience   The University of Western Ontario
2013-2015

Research Assistant
The University of Western Ontario
2013-2015